MODELING OCCLUSION AND SCALING IN NATURAL IMAGES

YANN GOUSSEAU* AND FRANÇOIS ROUEFF*

Abstract. The dead leaves model, introduced by the Mathematical Morphology school, consists of the superposition of random closed sets (the objects), and enables to model the occlusion phenomena. When combined with specific size distributions for objects, one obtains random fields providing adequate models for natural images. However, this framework imposes bounds on the sizes of objects. We consider the limits of these random fields when letting the cutoff sizes tend to zero and infinity. As a result we obtain a random field that contains homogeneous regions, satisfies scaling properties and is statistically relevant for modeling natural images. We then investigate the combined effect of these features on the regularity of images in the framework of Besov spaces.

Key words. occlusion, power laws, dead leaves model, natural images, Besov spaces

AMS subject classifications. Primary 60G18, 60G60, 60D05. Secondary 62M40

1. Introduction and motivations. Spatial statistics of natural images exhibit non-gaussianity, as well as scaling properties. These two phenomena may for instance be easily observed on the distribution of the gradient of images gray levels. Other quantities bearing these properties include the power spectrum (see [33] and the references therein), wavelet coefficients ([38], [20]) and morphological quantities ([2]). Classical mathematical models usually fail short of accounting for all these observations. For instance, Markov Random Fields (see [16, 43]) do not handle scaling properties properly and scale invariant Gaussian models fail to capture the structure of natural images, see [28]. Additive models (random wavelet expansions or template based models, see e.g. [39]) enable to simultaneously capture scaling properties and non-Gaussianity but imply intricate modelings in order to handle geometric structures, see e.g. [7, 31]. Indeed, the motivation behind this class of models is mainly of an algorithmic nature, and is not driven by the mechanisms of natural images formation. In this paper, we choose to start from a simplified modeling of the formation of natural images and investigate the effect of scaling behaviors in this context.

Non-gaussianity is strongly related to the occlusion phenomenon. Indeed, in the process of image formation, objects hide themselves depending on where they lie with respect to the camera, which differs totally from an additive generation. This phenomenon leads to peculiar geometrical structures such as homogeneous regions, borders and T-junctions. G. Matheron has proposed a framework to study this aspect of image formation, the *dead leaves* model, [24], consisting in the sequential superposition of random objects on the plane. Despite some limitations (objects are assumed independent, their size does not depend on the distance to the observer), it provides a simple model for the formation of a natural scene made of opaque objects. Let us mention at this point that the mere nature of the model enables the reproduction of characteristic structures of natural images such as one-dimensional discontinuities and homogeneous regions. Next, we take interest in the implications of the simultaneous modeling of occlusion and scaling properties on the regularity of images. It is therefore quite natural to impose a power law $x^{-\alpha}$ for the distribution of the size x of objects in a dead leaves model (note that such a distribution of object sizes was also considered in [9], but without occlusion). In fact, several studies ([34], [2], [22]) show that meaningful natural images statistics (linear or not) may be reproduced by

*TSI / CNRS UMR 5141, Ecole Nationale Supérieure des Télécommunications, 46 rue Barrault, 75634, Paris Cedex 13, France (`[gousseau,roueff]@tsi.enst.fr`)

such a model. In [22], a version of the model corresponding to strict scale invariance is considered (that is $\alpha = 3$) whereas [34] and [2] consider α as a parameter of the model. In both cases, a crucial assumption is that sizes of objects stay between two positive *cutoff* scales. Our goal is to investigate the small scale regularity of images when one extends the model to allow for the presence of details at arbitrary small scales.

In this paper, we define a new model for natural images, obtained by letting the lower cutoff scale of a dead leaves model tend to zero while keeping scaling properties. By doing this, we model the small scales properties of natural images in a non-trivial way. We are then in a position to study the regularity of images from a functional analysis point of view.

2. Detailed outline. In this section, we summarize the construction and main properties of the random field that we suggest for image modeling.

Basic definitions (Section 3). We recall some definitions and results on random closed sets, random tessellations and *colored* (or *textured*) tessellations. We also recall the definition of the dead leaves model, a tessellation obtained by superimposing "random objects" (see Figure 3.1). Formally, these objects are independent and identically distributed (i.i.d.) random closed sets $\{X_i\}$, satisfying mild geometric assumptions. The elements of the corresponding partition of the plane (uniform regions in Figure 3.1) are called the visible parts, $\{V_i\}$.

A dead leaves model with scaling properties (Section 4). As explained in the introduction, motivated by empirical observations on natural images, we choose objects sizes distributed according to a power law $r^{-\alpha}$ with exponent $\alpha > 1$. In order for this model to be well defined, one has to impose minimum and maximum sizes r_0 and r_1 for the objects, such that $0 < r_0 < r_1 < \infty$ if $\alpha \in (1, 3]$ and $0 < r_0 < r_1 \leq \infty$ if $\alpha > 3$. The obtained tessellation is denoted by $M(r_0, r_1)$. The main question we will address in this paper is *what happens when we let the small cutoff scale, r_0, tends to zero ?* A first result (Proposition 4.2) is that, whatever α may be, the boundary of $M(r_0, r_1)$ tends to $\mathbb{R}^2$, in the sense of the weak convergence of closed sets. Intuitively, this means that there are small objects everywhere on the plane. The limit boundary set is not the right way to describe a potential limit model.

The limit SDL model (Section 5). We then consider the random field I, a *colored random tessellation* that is obtained by independently and identically coloring each visible part V_i. Such a random field will be studied trough its finite-dimensional distributions. We consider limits of I as r_0 tends to 0, and also as r_1 tends to infinity. Under mild regularity assumptions on the objects X_i, and writing $\xrightarrow{\text{fidi}}$ for the convergence in the sense of finite-dimensional distributions, we get (Propositions 5.1 and 5.6, Theorem 5.4 and Remark 2) that

(1) If $\alpha > 3$, then $I \xrightarrow{\text{fidi}} W$ as $r_0 \to 0$ for all $r_1 \in (0, \infty]$, where W is white noise,
(2) if $\alpha < 3$, then $I \xrightarrow{\text{fidi}} C$ as $r_1 \to \infty$ for all $r_0 > 0$, where C is a constant field,
(3) If $\alpha < 3$, then $I \xrightarrow{\text{fidi}} \tilde{I}$ as $r_0 \to 0$ for all $r_1 > 0$, where $\tilde{I}$ is a measurable and stochastically continuous random field.

Cases (1) and (2) are degenerate (the case $\alpha = 3$ is degenerate too), and the case of most interest is case (3). We call $\tilde{I}$ a scaling dead leaves model (SDL). An interesting property of the SDL is that its finite-dimensional distributions may be expressed as mixtures (Corollary 5.5), whose weights are given by geometrical properties of the objects X_i's. Despite the presence of small objects everywhere, the bivariate distributions is coherent with the presence of homogeneous regions and discontinuities observed in natural images (see Figure 5.2).

Smoothness properties of the limit model (Section 6). Eventually we take interest in the small scales structure of the SDL $\tilde{I}$, in the framework of Besov spaces. Assuming that $2 < \alpha < 3$, a range of values that corresponds to observations on natural images, we show (Proposition 6.2) that

$$E\left[|\tilde{I}|^p_{B^{s,p}_p}\right] < \infty \Leftrightarrow s < \frac{3-\alpha}{p}.$$

This results gives a quantitative measure of natural images irregularity (sometimes called *clutter*) from a functional analysis point of view. In particular, writing $|.|_{BV}$ for the bounded variation norm, it is easily derived that $E|\tilde{I}|_{BV} = \infty$, which is in agreement with experimental observations. We conclude by discussing the links between the regularity of the SDL and classical $u+v$ models (Section 7), as well as its potential use as a Bayesian prior (Section 8).

3. Basic definitions.

3.1. Closed sets.

Let $\mathcal{F}$ and $\mathcal{K}$ be respectively the sets of all closed and compact sets of $\mathbb{R}^2$, endowed with the "hit or miss" topology, see [25]. We write $\mathcal{B}_{\mathcal{F}}$ for the associated Borel σ-field. An interesting fact is that $\mathcal{B}_{\mathcal{F}}$ is generated by the family $\{\mathcal{F}_K, K \in \mathcal{K}\}$, where

$$\mathcal{F}_K = \{F \in \mathcal{F} \,:\, F \cap K \neq \emptyset\}.$$

A random closed set (RACS) of $\mathbb{R}^d$ is defined as a measurable function from a probability space to $(\mathcal{F}, B_{\mathcal{F}})$.

Classical operations of Mathematical Morphology are measurable functions in this setting. For any sets A and B, we will denote

$$\begin{aligned}
\check{A} &= \{-x, x \in A\},\\
A \ominus B &= \{x \in \mathbb{R}^d,\, x + \check{B} \subset A\},\\
A \oplus B &= \{x + y, x \in A, y \in B\},
\end{aligned}$$

$A \ominus \check{B}$ is called the erosion of A by B and $A \oplus \check{B}$ the dilation of A by B.

3.2. σ-finite and counting measures on $\mathcal{F}'$.

Following [25] we define a σ-finite measure on $\mathcal{F}' := \mathcal{F}\backslash\{\emptyset\}$ as a measure which is finite on $\mathcal{F}_K$ for all $K \in \mathcal{K}$. We denote by $\mathcal{N}_{\mathcal{F}'}$ the set of σ-finite counting measures on $(\mathcal{F}', \mathcal{B}_{\mathcal{F}'})$. For all $\mu \in \mathcal{N}_{\mathcal{F}'}$, we write $\mu = \sum_i \delta_{F_i}$, where δ_{F_i} denotes the unit mass measure at point F_i. We further denote by $\mathcal{B}_{\mathcal{N}_{\mathcal{F}'}}$ its usual σ-field (that is, the smallest one such that, for all compact set $A \in \mathcal{B}_{\mathcal{F}'}$, the $\mathcal{N}_{\mathcal{F}'} \to \mathbb{N}$ function $\mu \mapsto \mu(A)$ is measurable). A point process on $\mathcal{F}'$ is then defined as a measurable function from a probability space to $(\mathcal{N}_{\mathcal{F}'}, \mathcal{B}_{\mathcal{N}_{\mathcal{F}'}})$.

3.3. Tessellations.

Intuitively, a tessellation is a collection of cells which partition the plane. It is in fact convenient to define a tessellation as a point process on closed sets along the same lines as the so called *generalized tessellations* introduced in [40] (see also [6]).

Definition 3.1. *Let $T = \sum_i \delta_{F_i} \in \mathcal{N}_{\mathcal{F}'}$. We say that T is a tessellation if*

(i) $\bigcup_i F_i = \mathbb{R}^d$.

(ii) for all $i \neq j$, $\overset{\circ}{F}_i \cap F_j = \emptyset$, *where* $\overset{\circ}{F}$ *denotes the interior of* F.

The sets F_is are called the cells *of the tessellation T. We also define the* boundary set *of T by $\partial T := \cup_i \partial F_i$.*

In fact, (i) and (ii) are equivalent to saying that $\{\partial T, (\overset{\circ}{F}_i)_i\}$ is a partition of $\mathbb{R}^2$. Classical examples of random tessellations (see the references in [41, Chapter 10]) include Poisson hyperplanes processes, Delaunay, Voronoi and Johnson-Mehl tessellations, and the dead leaves model that we consider below.

By analogy with Definition 2-5-2 in [25], we will say that a random tessellation T defined on a probability space $(\Omega, \mathcal{S}, \mathbb{P})$ is *a.s. continuous* if

$$\mathbb{P}(\mathbf{x} \in \partial T) = 0 \quad \text{for all } \mathbf{x} \in \mathbb{R}^2. \tag{3.1}$$

This property holds under minimal assumptions on the F_i's. For instance, it is automatically satisfied if T is stationary and if, for all i, $\nu(\partial F_i) = 0$, where ν is the 2-dimensional Lebesgue measure.

3.4. Colored tessellations. From a tessellation one may define a random field by independently "coloring" (or texturing) each cell of a random tessellation.

DEFINITION 3.2. *Let $T = \sum_i \delta_{F_i}$ and $\mathcal{C} = \{\mathcal{C}(\mathbf{x}) : \mathbf{x} \in \mathbb{R}^d\}$ be a random tessellation and a real valued random field, respectively. Let $\{\mathcal{C}_i\}$ be a collection of i.i.d. random fields with same distribution as $\mathcal{C}$ and independent of T. The random field I defined by*

$$I(\mathbf{x}) = \sum_i \mathbb{1}(\mathbf{x} \in \overset{\circ}{F}_i)\, \mathcal{C}_i(\mathbf{x}), \quad \mathbf{x} \in \mathbb{R}^d\ ,$$

is called the colored tessellation field *associated to T and $\mathcal{C}$.*

Since T is a tessellation, I satisfies

$$\begin{cases} I(\mathbf{x}) = \mathcal{C}_{i(\mathbf{x})}(\mathbf{x}) & \text{for all } \mathbf{x} \in \bigcup_i \overset{\circ}{F}_i, \\ I(\mathbf{x}) = 0 & \text{for all } \mathbf{x} \in \partial T, \end{cases}$$

where, for all $\mathbf{x} \in \bigcup_i \overset{\circ}{F}_i$, $i(\mathbf{x})$ denotes the unique index such that $\mathbf{x} \in \overset{\circ}{F}_{i(\mathbf{x})}$. If T is a.s. continuous, $\mathbf{x}$ has probability zero to fall on ∂T so that $I(\mathbf{x})$ has the same marginal distribution as $\mathcal{C}(\mathbf{x})$.

Remark 1. *The simplest way of coloring a tessellation is to take a constant field for $\mathcal{C}$, that is to attach i.i.d. random colors $\mathcal{C}_i \in \mathbb{R}$ to the F_i's. Images displayed in the present paper have been simulated this way. In this simple case, it is easily seen that in order to recover T from I a different color should be assigned to each F_i, that is, the distribution of $\mathcal{C}$ should not have point masses.*

We now introduce Bernoulli processes that will be used for computing the finite-dimensional distributions of I.

DEFINITION 3.3. *Let $T = \sum_i \delta_{F_i}$ be a random tessellation. For all $\mathbf{x}, \mathbf{y} \in \mathbb{R}^d$, let $R(\mathbf{x}, \mathbf{y})$ denote the (Bernoulli) random variable which takes value one if there exists i such that the points $\mathbf{x}$ and $\mathbf{y}$ are in $\overset{\circ}{F}_i$ and takes value zero otherwise, that is*

$$R(\mathbf{x}, \mathbf{y}) := \sum_i \mathbb{1}(\{\mathbf{x}, \mathbf{y}\} \subset \overset{\circ}{F}_i), \quad \mathbf{x}, \mathbf{y} \in \mathbb{R}^d. \tag{3.2}$$

We will call $\{R(\mathbf{x}, \mathbf{y}) : (\mathbf{x}, \mathbf{y}) \in \mathbb{R}^d \times \mathbb{R}^d\}$ the partition process.

Clearly the finite dimensional distributions of the partition process R and of the random field $\mathcal{C}$ are sufficient to determine the finite dimensional distributions of I. For instance, a direct computation shows that, for all $\mathbf{x}, \mathbf{y} \in \mathbb{R}^d$, the bivariate distribution $(I(\mathbf{x}), I(\mathbf{y}))$ has the same distribution as the mixture

$$R(\mathbf{x}, \mathbf{y})\,(\mathcal{C}(\mathbf{x}), \mathcal{C}(\mathbf{y})) + (1 - R(\mathbf{x}, \mathbf{y}))\,(\mathcal{C}(\mathbf{x}), \mathcal{C}'(\mathbf{y})) \tag{3.3}$$

where $\mathcal{C}'$ is a copy of $\mathcal{C}$ and $\mathcal{C}$, $\mathcal{C}'$ and R are mutually independent. It turns out that all finite-dimensional distributions have similar mixture structures as described in Appendix A. In this appendix we also give simple criteria for the finite-dimensional convergence of such fields.

3.5. The dead leaves model. The dead leaves model (see [24], [37], [10], [21], [6]) is a particular instance of a random tessellation of the plane, obtained through sequential superposition of random objects falling on the plane. As explained in the introduction, it is a simplified model for the formation of images, accounting for occlusion. More formally, let X be a random closed set. Let $\Phi := \sum_i \delta_{\mathbf{x}_i, t_i, X_i}$ be a point process on a probability space $(\Omega, \mathcal{S}, \mathbb{P})$, such that $\sum_i \delta_{\mathbf{x}_i, t_i}$ is a homogeneous Poisson point process on $\mathbb{R}^2 \times (-\infty, 0]$ with intensity one, and $\{X_i\}$ are i.i.d. closed sets with the same distribution as X, independent of $\sum_i \delta_{\mathbf{x}_i, t_i}$.

DEFINITION 3.4. *The random closed set $\mathbf{x}_i + X_i$ is called a leaf and*

$$V_i := (\mathbf{x}_i + X_i) \setminus \left(\bigcup_{t_j \in (t_i, 0)} \left(\mathbf{x}_j + \overset{\circ}{X}_j \right) \right) \tag{3.4}$$

is called a visible part.

V_i is what remains visible from the object X_i once it has been covered by objects falling at times larger than t_i.

In the sequel, we let ν denote the Lebesgue measure on $\mathbb{R}^2$, E the integration with respect to the distribution of X (in contrast, $\mathbb{E}$ will denote the expectation with respect to $\mathbb{P}$) and we assume that,

(C-1) for all $K \in \mathcal{K}$, $E\nu(X \oplus K) < \infty$,

(C-2) X is a regular closed set, that is, X is the closure of its interior a.s.,

(C-3) there exists $a > 0$ such that $E\nu(X \ominus D(a)) > 0$,

where $D(a)$ is the disk of radius a centered at the origin. Under these assumptions, it can be shown (see [6]) that $M := \sum_i \mathbb{1}(\overset{\circ}{V}_i \neq \emptyset)\delta_{V_i}$ is a stationary random tessellation of $\mathbb{R}^2$. Hence the following definition.

DEFINITION 3.5. *The tessellation $M = \sum_i \mathbb{1}(\overset{\circ}{V}_i \neq \emptyset)\delta_{V_i}$ is the dead leaves model associated with the distribution of X.*

The main practical result from [24] concerns a functional defined on the set of compact sets of the plane, equal to the probability that a given compact is included in the interior of a visible part of the model:

$$Q(K) := \mathbb{P}(\exists t_i \leq 0 : K \subset \overset{\circ}{V}_i), \quad K \in \mathcal{K}.$$

$$Q(K) = \frac{E\nu(\overset{\circ}{X} \ominus \check{K})}{E\nu(X \oplus \check{K})}. \tag{3.5}$$

In Appendix B, we give a generalization of this result, proved in [6], which allows to compute the finite dimensional distributions of a colored dead leaves model.

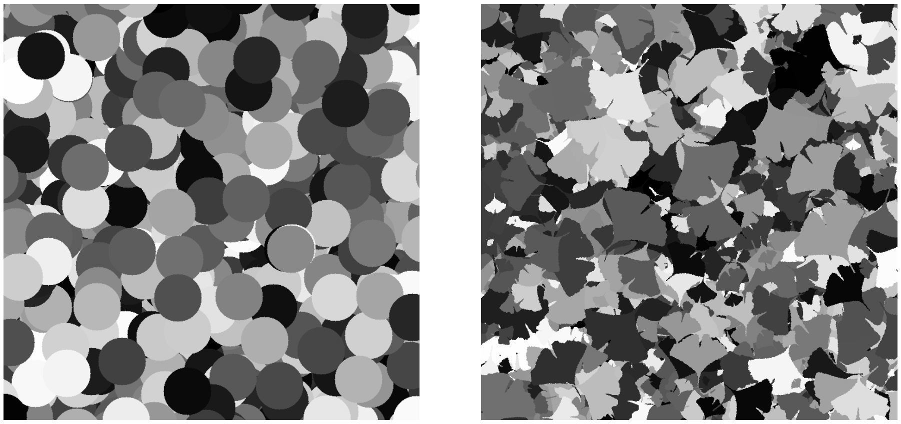

FIGURE 3.1. *Two examples of dead leaves models. Left, random objects are disks with a deterministic radius. Right, objects are homothetics of a reference shape, with uniformly distributed ratio.*

4. A dead leaves model with scaling properties. We now take interest in a dead leaves model defined by using a specific object distribution for X. Namely we choose for X the homothetic of a random compact set Y, that is $X = RY$, where R is a positive random variable independent of Y. Hence E now denotes integration with respect to the joint distribution of (R, Y). We will consider in details the case where R has probability density defined by

$$f_{r_0,r_1}(r) = \eta(r_0, r_1)\, r^{-\alpha}\, \mathbb{1}(r_0 < r < r_1), \tag{4.1}$$

where $0 < r_0 < r_1$, $\alpha > 1$ and where the normalizing constant reads

$$\eta(r_0, r_1) = (1-\alpha)^{-1}(r_0^{1-\alpha} - r_1^{1-\alpha}). \tag{4.2}$$

For convenience, our notations do not refer to the scaling parameter α. However, it must be kept in mind that these definitions highly depend on this parameter. For R to correspond to a meaningful scale of X, we want to keep Y within fixed proportions. Hence the assumption

(A-1) there exist $a_2 > a_1 > 0$ such that, a.s, $D(a_1) \subset Y \subset D(a_2)$.

The density chosen above for R indicates that the size distribution of objects satisfies some scaling properties within a given range imposed by r_0 and r_1. This choice for f_{r_0,r_1} is motivated by natural images modeling, see [34], [2], [22]. Since $\alpha > 1$ we cannot take $r_0 = 0$ for f_{r_0,r_1} to be a density. Now, taking $r_0 > 0$ is not satisfying as well. From a theoretical point of view, this reduces the model to only very simple smoothness classes (namely, piecewise constant images). From a practical point of view, it means that there exists a minimal size for the objects in the image. It is not clear at all what physical meaning to give to this minimum objects size, and how to deal with this supplementary parameter of the model. It is also unclear how to relate this minimum size to the resolution of a digital image, e.g. obtained by filtering and subsampling a realization of the model. Moreover, this contradicts empirical experiments (see [17]) which conclude to the presence of small *objects* up to the smallest observable scales in digital images. Therefore it is worthwhile to wonder about the limit of the model as r_0 tends to zero. The parameter r_1 is not crucial for modeling smoothness properties because it does not influence the small scales behavior, except perhaps when $r_1 = \infty$ or r_1 tends to infinity, in which case the model may degenerate.

For X to satisfy (C-2), we will impose the same condition on Y, namely

(A-2) Y is a regular closed set a.s.

We further consider the following assumption which holds in standard cases.

(A-3) $\nu(\partial Y) = 0$ a.s.

Observe that none of these last two assumptions implies the other one, see [6]. Applying [6], we have the following:

PROPOSITION 4.1. *Let $r_0 > 0$ and assume either $r_1 \in (r_0, \infty)$ and $\alpha \in (1, 3]$, or $r_1 \in (r_0, \infty]$ and $\alpha > 3$. Under (A-1) and (A-2), $X = RY$ satisfies (C-1), (C-2) and (C-3). We denote by $M(r_0, r_1)$ the corresponding dead leaves model. Moreover, under (A-3), $M(r_0, r_1)$ is a.s. continuous.*

From now on, we always assume that Y satisfies (A-1), (A-2) and (A-3).

At fixed α and at fixed distribution for Y, Proposition 4.1 then provides a range of values for (r_0, r_1) defining a.s. continuous random tessellations $M(r_0, r_1)$.

We now come to the convergence of $M(r_0, r_1)$. In this section we take the classical point of view of random closed sets and we consider the distribution of the (random) boundary set $\partial M(r_0, r_1)$ (see Definition 3.1). It turns out that it has a degenerate limit as r_0 decreases to zero. Intuitively, this means that there are small objects everywhere on the plane.

PROPOSITION 4.2. *Take $M(r_0, r_1)$ as defined in Proposition 4.1. Then*

$$\lim_{r_0 \to 0} \partial M(r_0, r_1) = \mathbb{R}^2,$$

where the limit is meant in the sense of the weak convergence of random closed sets.

This convergence result follows from the next lemma which investigates the presence of constant areas as r_0 tends to zero, at fixed α and r_1.

LEMMA 4.3. *Let $Q(r_0, r_1, r)$ denote the probability for a disk of radius r to be included in the interior of a visible part of $M(r_0, r_1)$. Then, for any $r > 0$, $\lim_{r_0 \to 0} Q(r_0, r_1, r) = 0$.*

Proof. According to formula (3.5) and then to (A-1), we have, for all sufficiently small $r_0 > 0$,

$$Q(r_0, r_1, r) = \frac{E\nu(\overset{\circ}{X} \ominus D(r))}{E\nu(X \oplus D(r))} \leq \frac{E\nu(RD(a_2) \ominus D(r))}{E\nu(RD(a_1) \oplus D(r))} = \frac{\int_{a_2^{-1} r}^{r_1} \pi(ua_2 - r)_+^2 \, u^{-\alpha} \, du}{\int_{r_0}^{r_1} \pi(ua_1 + r)^2 \, u^{-\alpha} \, du}.$$

The limit is now obvious. $\square$

Proof of Proposition 4.2. Let $P(r_0, r_1, \cdot)$ denote the probability law of $\partial M(r_0, r_1)$ in the probability space $(\mathcal{F}, B_\mathcal{F})$. We recall that a sequence P_n weakly converges to P in $(\mathcal{F}, B_\mathcal{F})$ if for all $E \in B_\mathcal{F}$ such that $P(E) = P(\overset{\circ}{E})$, $P_n(E)$ converges to $P(E)$ (see [5]). Moreover, in the case of the probability space $(\mathcal{F}, B_\mathcal{F})$, this amounts to check that for all $K \in \mathcal{K}$ such that $P(\mathcal{F}_K) = P(\mathcal{F}_{\overset{\circ}{K}})$, $P_n(\mathcal{F}_K)$ converges to $P(\mathcal{F}_K)$ (see [23], [27]). Here the limit distribution P associated with the deterministic set $\mathbb{R}^2$ satisfies $P(\mathcal{F}_K) = 1$ for all compact set $K \neq \emptyset$ and $P(\mathcal{F}_\emptyset) = 0$. Take a compact set K such that $\overset{\circ}{K} \neq \emptyset$. Then there exists a disk with positive radius r included in K so that

$$P(r_0, r_1, \mathcal{F}_K) \geq P(r_0, r_1, \mathcal{F}_{D(r)}) = 1 - Q(r_0, r_1, r).$$

The result then follows from Lemma 4.3. ∎

5. The colored dead leaves process and its limit. We saw above that, from the point of view of random closed sets, the limit of $\partial M(r_0, r_1)$ as $r_0 \to 0$ degenerates. We thus take interest in the limit of a colored dead leaves model in the sense of finite-dimensional distributions. In this context, we will also investigate the limit as $r_1 \to \infty$.

We proceed in two steps. First, we investigate the limits of the marginal distribution of R_{r_0,r_1}, defined as the partition process (see Definition 3.3) of M_{r_0,r_1}. Depending on the value of α, these limits will degenerate as $r_0 \to 0$ or $r_1 \to \infty$. Second, we focus on the interesting cases and derive the limits of the colored field.

5.1. Basic convergence results. Let $p(r_0, r_1, \mathbf{x})$ denote the probability that the origin and $\mathbf{x} \in \mathbb{R}^2$ are in the same visible part of the dead leaves model $M(r_0, r_1)$. By stationarity of $M(r_0, r_1)$, its partition process satisfies

$$\mathbb{P}\{R_{r_0,r_1}(\mathbf{x}, \mathbf{y}) = 1\} = p(r_0, r_1, \mathbf{y} - \mathbf{x}), \quad \mathbf{x}, \mathbf{y} \in \mathbb{R}^2. \tag{5.1}$$

Let us now compute this probability. According to (3.5) and since, by (A-3), $\nu(\partial X) = 0$ a.s., for all $\mathbf{x} \in \mathbb{R}^2$,

$$p(r_0, r_1, \mathbf{x}) = \frac{E\nu\left(X \ominus \{0, \mathbf{x}\}\right)}{E\nu\left(X \oplus \{0, \mathbf{x}\}\right)} = \frac{E\nu\left(X \cap (\mathbf{x} + X)\right)}{E\nu\left(X \cup (\mathbf{x} + X)\right)}.$$

Fubini's Theorem and the homogeneity of ν give

$$\begin{aligned} E\nu\left(X \cap \mathbf{x} + X\right) &= \int_{r_0}^{r_1} E\nu\left(uY \cap (\mathbf{x} + uY)\right) \, f_{r_0,r_1}(u) \, du \\ &= \eta(r_0, r_1) \int_{r_0}^{r_1} \gamma\left(\frac{\mathbf{x}}{u}\right) \, u^{2-\alpha} \, du, \end{aligned}$$

where γ denotes the geometric covariogram of Y, see [25], that is, for all $\mathbf{y} \in \mathbb{R}^2$,

$$\gamma(\mathbf{y}) := E\nu\left(Y \cap (\mathbf{y} + Y)\right).$$

Since

$$\nu\left(X \cup (\mathbf{x} + X)\right) = \nu\left(X \cup (\mathbf{x} + X)\right) = 2\nu\left(X\right) - \nu\left(X \cap \mathbf{x} + X\right),$$

we finally obtain, for all $\mathbf{x} \in \mathbb{R}^2$,

$$p(r_0, r_1, \mathbf{x}) = \frac{\int_{r_0}^{r_1} \left[\gamma(0) + (\gamma(\mathbf{x}/u) - \gamma(0))\right] u^{2-\alpha} \, du}{\int_{r_0}^{r_1} \left[\gamma(0) - (\gamma(\mathbf{x}/u) - \gamma(0))\right] u^{2-\alpha} \, du}. \tag{5.2}$$

From (5.1) and (5.2), we see that the marginals of the partition process may be expressed using r_0, r_1, α and the functional γ which only depends on the distribution of Y. We apply (5.2) and investigate the limits of $p(r_0, r_1, \cdot)$ as one pushes the model towards the values of r_0 and r_1 which are not allowed, that is, for all $1 < \alpha \leq 3$, $r_1 \to \infty$, in which case Condition (C-1) does not hold, and, for all $\alpha > 1$, $r_0 \to 0$ in which case $f_{0,r_1}(\cdot)$ is not a density. The proof of the following result is postponed to Appendix D.1.

PROPOSITION 5.1. *We have the following limits for $p(r_0, r_1, x)$.*

(i) *for all* $1 < \alpha < 3$ *and* $\mathbf{x} \in \mathbb{R}^2$, $\lim_{r_1 \to \infty} \inf_{r_0 \in (0,r_1)} p(r_0, r_1, \mathbf{x}) = 1$,

(ii) *for all* $\alpha > 3$ *and* $\mathbf{x} \neq 0$, $\lim_{r_0 \to 0} \sup_{r_1 \in (r_0,\infty]} p(r_0, r_1, \mathbf{x}) = 0$,

(iii) *for all* $\alpha = 3$ *and* $\mathbf{x} \neq 0$, $\lim_{\substack{r_0 \to 0 \\ r_1 \to \infty}} \left[p(r_0, r_1, \mathbf{x}) \left(1 - 2\frac{\log(r_0)}{\log(r_1)} \right) \right] = 1$.

(iv) *for all* $\alpha \in (1,3)$, $r_1 \in (0,\infty)$ *and* $\mathbf{x} \in \mathbb{R}^2$, $\lim_{r_0 \to 0} p(r_0, r_1, \mathbf{x}) = p(0, r_1, \mathbf{x})$, *where*

$$p(0, r_1, \mathbf{x}) := \frac{\displaystyle\int_0^{r_1} \gamma(\mathbf{x}/u)\, u^{2-\alpha}\, du}{\displaystyle\int_0^{r_1} (2\gamma(0) - \gamma(\mathbf{x}/u))\, u^{2-\alpha}\, du} \tag{5.3}$$

is a continuous function of $x \in \mathbb{R}^2$.

It is worth elaborating on these simple convergence results. In case (i), as $r_1 \to \infty$, however $r_0 < r_1$ may behave, any two points end up in the same visible part; the big objects predominate at the limit. In case (ii), the result is the exact opposite. As $r_0 \to 0$, however $r_1 \in (r_0, \infty]$ may behave, any two distinct points never belong to the same object; the small objects predominate. See Figure 5.1 for an illustration of these cases. In case (iii), the limit depends on the behavior of $\log(r_0)/\log(r_1)$. Convergence to 1 or 0 as in cases (i) and (ii) are observed if only one of the limit $r_0 \to 0$ or $r_1 \to \infty$ is taken. Now, if for instance we take $r_0 = r_1^{-s}$ for a fixed s, and let r_1 tend to ∞, we obtain a limit which depends on s but does not depend on x.

Remark 2. *Using Corollary A.3 in Appendix A, one shows that in cases (i) and (ii) of Proposition 5.1 the colored dead leaves model converges to a constant field and a white noise, respectively. Case (iii) is more involved but can be shown to converge to a mixture of a constant field and a white noise with weights depending on the limit of* $\log(r_0)/\log(r_1)$.

We will avoid cases (i), (ii) and (iii) in the sequel as they give uninteresting limits. In contrast, case (iv) defines a non-degenerate prolongation of $p(r_0, r_1, \cdot)$ at $r_0 = 0$. In the following result, by assuming sufficient smoothness on the boundary of Y, we provide simple approximations as $|\mathbf{x}| \to 0$ in which the geometry of the model only appears in multiplicative constants, while the qualitative behavior is a power law of $|\mathbf{x}|$ with exponent only depending on α. For the sake of completeness we also study $p(r_0, \infty, \mathbf{x})$ when $\mathbf{x} \to \infty$. In order to simplify these results, we temporarily assume that the distribution of Y is isotropic. However, in the case of non-isotropic Y, the various quantities under study can be adapted by introducing a directional parameter. In the isotropic case, we let γ and $p(r_0, r_1, \cdot)$ be functions of the real variable $x = |\mathbf{x}|$. The proof of the following result is postponed to Appendix D.2.

PROPOSITION 5.2. *We have the following asymptotic equivalences.*

(i) *For all* $\alpha > 3$, $p(r_0, \infty, x) \sim g_1(\alpha)\, (x/r_0)^{3-\alpha}(1 + o(1))$ *as* $x/r_0 \to \infty$, *where*

$$g_1(\alpha) := \frac{\alpha - 3}{2\gamma(0)} \int_0^\infty \gamma(1/v)\, v^{2-\alpha}\, dv < \infty.$$

(ii) *For all* $\alpha \in (2,3)$, *if*

$$g_2(\alpha) := \frac{2(3-\alpha)}{\gamma(0)} \int_0^\infty (\gamma(0) - \gamma(1/v))\, v^{2-\alpha}\, dv < \infty\ , \tag{5.4}$$

then $1 - p(0, r_1, x) \sim g_2(\alpha)\, (x/r_1)^{3-\alpha}$ *as* $x/r_1 \to 0$.

The condition on g_2 in (5.4) depends on the behavior of γ at the origin. For instance, it is satisfied for any $\alpha > 2$ if

(A-4) For any $\delta > 0$, we have $\gamma(\mathbf{x}) = \gamma(0) + o(|\mathbf{x}|^{1-\delta})$ when $\mathbf{x} \to 0$.

The scope of validity of this assumption and how it relates to geometric properties of Y is investigated in Appendix C.

Remark 3. *If $\alpha \in (1, 2]$ it is easily seen that the behavior of $1 - p(0, r_1, x)$ as $x/r_1 \to 0$ depends on the derivative of γ at the origin. If the right-sided derivative of $x \mapsto \gamma(x)$ exists, then $1 - p(0, r_1, x)$ behaves as $(x/r_1)\log(x/r_1)$ for $\alpha = 2$, and as (x/r_1) for $\alpha \in (1, 2)$.*

Case (i) and (ii) exhibit power laws at small and large scales, that is when x is much smaller than the cutoff scale r_1, and much larger than r_0, respectively. We will see in the end of Section 5.2 how these power laws relate to second order properties of natural images.

5.2. Limit field at small scales. From now on we assume that

$$\text{either } 1 < \alpha \leq 3 \text{ and } r_1 > 0, \text{ or } \alpha > 3 \text{ and } r_1 \in (0, \infty].$$

DEFINITION 5.3. *Let $\mathcal{C} := \{\mathcal{C}(\mathbf{x}),\, \mathbf{x} \in \mathbb{R}^2\}$ be a random field. We denote by $I_{r_0}^{\mathcal{C}}$ the colored dead leaves model obtained from the random tessellation $M(r_0, r_1)$ (see Definition 3.2).*

If $\mathcal{C}$ is the constant random field with uniform marginals, that is, for all $\mathbf{x_1}, \ldots, \mathbf{x_n}$, $\mathcal{C}(\mathbf{x_1}) = \cdots = \mathcal{C}(\mathbf{x_n})$ is uniformly distributed on $[0, 1]$, we simply denote the colored dead leaves model by I_{r_0}. In other words I_{r_0} is obtained from the dead leaves model by independently coloring each leaf with a uniform distribution.

Remark 4. *Observe that, if $\mathcal{C}$ is a stationary field, then the same is true for $I_{r_0}^{\mathcal{C}}$. For instance, I_{r_0} is stationary.*

We now investigate the existence of a continuous prolongation of $I_{r_0}^{\mathcal{C}}$ at $r_0 = 0$. Simple conditions for the convergence of colored tessellations are given in Appendix A, see Proposition A.1. These conditions involve the partition process of $I_{r_0}^{\mathcal{C}}$ (see Definition 3.3), which we now denote by $\{R_{r_0}(\mathbf{x}, \mathbf{y}) : \mathbf{x}, \mathbf{y} \in \mathbb{R}^2\}$.

Let us recall that, for a sequence of random fields $\{I_j\}$, we say that I_j converges to a random field I_∞ in the sense of finite-dimensional distributions, $I_j \xrightarrow{\text{fidi}} I_\infty$, if, for all $n \geq 1$ and for all $\mathbf{x_1}, \ldots \mathbf{x_n} \in \mathbb{R}^d$, $(I_j(\mathbf{x_1}), \ldots, I_j(\mathbf{x_n}))$ converges to $(I_\infty(\mathbf{x_1}), \ldots, I_\infty(\mathbf{x_n}))$ in distribution.

THEOREM 5.4. *There exists a random field $I_0^{\mathcal{C}}$ such that*

$$I_{r_0}^{\mathcal{C}} \xrightarrow{\text{fidi}} I_0^{\mathcal{C}} \text{ as } r_0 \to 0.$$

Proof. Let $r_1 > 0$. In this proof, for all $r_0 \in (0, r_1)$, we denote by $\mathbb{P}_{r_0}$ the distribution of $M(r_0, r_1)$. Using Proposition A.1 in Appendix A, it is enough to prove that there exists a random process R_0 such that, as $r_0 \to 0$, $R_{r_0} \xrightarrow{\text{fidi}} R_0$. Since R_{r_0} is a field valued in $\{0, 1\}$, it is sufficient to show that, for all $n \geq 1$ and all $x_1, y_1, \ldots, x_n, y_n$ in the plan, $\mathbb{P}(R_{r_0}(x_1, y_1) = 1, \ldots, R_{r_0}(x_n, y_n) = 1)$ converges as $r_0 \to 0$. Recall that, for all x and y in the plane, $R_{r_0}(x, y) = 1$ is equivalent to say that $\{x, y\} \subset \overset{\circ}{V}_i$ for some visible part V_i of $M(r_0, r_1)$; thus, we now consider the probability $\mathbb{P}_{r_0}(\exists i_1, \ldots, i_n : K_1 \subset \overset{\circ}{V}_{i_1}, \ldots, K_n \subset \overset{\circ}{V}_{i_n})$ for fixed $n \geq 1$ and compact sets $K_1, \ldots, K_n$ and show that it converges in $[0, 1]$ as r_0 tends to 0. We may also assume without loss of generality that each K_j contains at least two distinct points.

Otherwise, since $M(r_0, r_1)$ is a.s. continuous, K_j is included in the interior of a visible part with probability one.

Finally, we claim that it is now enough to prove the convergence of

$$Q_{r_0}^{(n)}(K_1, \dots, K_n) := \mathbb{P}_{r_0}(\exists t_{i_1} < \cdots < t_{i_n} : K_1 \subset \overset{\circ}{V}_{i_1}, \dots, K_n \subset \overset{\circ}{V}_{i_n}).$$

This follows from the fact that the union of two compact sets is a compact set, so that we may restrict ourselves to disjoint visible parts, by an elementary induction. Following Proposition B.1 in Appendix B, we get that

$$Q_{r_0}^{(n)}(K_1, \dots, K_n) = F_{r_0}^{(n)}(K_1, \dots, K_n) / G_{r_0}^{(n)}(K_1, \dots, K_n), \tag{5.5}$$

where $F_{r_0}^{(n)}$ and $G_{r_0}^{(n)}$ are defined as in (B.1) and (B.2). Pick a K_j and let δ denote its diameter. Recall that we have assumed that it contains at least two distinct points so that $\delta > 0$. From (A-1), we have $\nu(RY \ominus \check{K}_j) = 0$ for all R such that $2Ra_2$ is smaller than δ. This implies that

$$\eta(r_0, r_1) E\nu\left((\overset{\circ}{X} \ominus \check{K}_j) \cap (X \oplus \underline{\check{K}}_{j-1})^{\mathrm{c}} \right) = \int_{r_0}^{r_1} E\nu\left((r\overset{\circ}{Y} \ominus \check{K}_j) \cap (rY \oplus \underline{\check{K}}_{j-1})^{\mathrm{c}} \right) r^{-\alpha}\, dr$$

stays constant as soon as r_0 goes below $\delta/(2a_2)$. Here, for $j \geq 1$, $\underline{\check{K}}_{j-1}$ is defined in (B.3), the case $j = 1$ being obtained with the convention $\underline{\check{K}}_0 = \emptyset$. Hence, from (B.1), it is clear that $F_{r_0}^{(n)}(K_1, \dots, K_n)\eta(r_0, r_1)^{-n}$ does not depend on r_0 for r_0 small enough. On the other hand, for all $j = 1, \dots, n$, we have

$$E\nu(\check{X} \oplus \underline{\check{K}}_j) = \eta(r_0, r_1) \int_{r_0}^{r_1} r^{-\alpha} E\nu\left(rY \oplus \underline{\check{K}}_j\right)\, dr.$$

Since the integrand is positive, $\eta(r_0, r_1)^{-n} G_{r_0}^{(n)}(K_1, \dots, K_n)$ has a limit in $(0, \infty]$ (it is non zero since the K_i's are non empty). Simplifying by $\eta(r_0, r_1)^{-n}$ in (5.5), we obtain that it has a limit as r_0 tend to the origin, which, as we claimed, is sufficient for showing Theorem 5.4. ∎

Note that in this result we did not separate the cases $\alpha < 3$ and $\alpha \geq 3$. However, in the latter case, the limit field is white noise (see Remark 2). In contrast, for $1 < \alpha < 3$, we will see in Proposition 5.6 that there exists a measurable version of the limit field allowing its functional analysis.

We conclude this section by a simple corollary of Theorem 5.4, where we compute the bivariate distributions of $I_{r_0}^{\mathcal{C}}$ for all $r_0 \in [0, r_1)$.

COROLLARY 5.5. *For all* $\mathbf{x}, \mathbf{y} \in \mathbb{R}^2$ *and for all* $r_0 \in [0, r_1)$, $(I_{r_0}^{\mathcal{C}}(\mathbf{x}), I_{r_0}^{\mathcal{C}}(\mathbf{y}))$ *is a mixture of the two (bivariate) random variables* $(\mathcal{C}(\mathbf{x}), \mathcal{C}(\mathbf{y}))$ *and* $(\mathcal{C}(\mathbf{x}), \mathcal{C}'(\mathbf{y}))$ *with respective weights* $p(r_0, r_1, \mathbf{y} - \mathbf{x})$ *and* $1 - p(r_0, r_1, \mathbf{y} - \mathbf{x})$, *where* $\mathcal{C}'$ *is an independent copy of* $\mathcal{C}$.

Proof. The case $r_0 > 0$ is given by (3.3) and (5.1). The case $r_0 = 0$ is obtained by applying Proposition 5.1 and Theorem 5.4. ∎

In particular, the covariance of a colored dead leaves model $I_{r_0}^{\mathcal{C}}$ is given by

$$\mathrm{cov}(I_{r_0}^{\mathcal{C}}(0), I_{r_0}^{\mathcal{C}}(\mathbf{x})) = p(r_0, r_1, \mathbf{x})\, \mathrm{var}(\mathcal{C}).$$

We have seen that, under minimal assumptions on Y and depending on the values of α, $p(r_0, r_1, \mathbf{x})$ exhibits power laws at large and small scales, see cases (i) and (ii) of Proposition 5.2 respectively. This kind of asymptotic results were already observed in [34] and served as a justification for introducing the distribution of objects given by (4.1). Indeed, experimental studies claim that the power spectrum of natural images is well approximated by a power function $S(\mathbf{f}) \sim |\mathbf{f}|^{-2+\eta}$, see [33]. It is known that, by using Tauberian results, such power law behavior, at low or high frequencies, relates to a power law behavior in the covariance function of the form $|\mathbf{x}|^{-\eta}$ at large scales or $|\mathbf{x}|^{-\eta}$ at small scales, respectively. Observe that a parallel can be drawn between conditions for S to be integrable ($\eta > 0$ at low frequencies and $\eta < 0$ at high frequencies), and conditions for $p(r_0, r_1, \mathbf{x})$ to be non-degenerate (see Section 5.1, $\alpha > 3$ for $r_1 = \infty$ and $\alpha < 3$ for $r_0 = 0$).

5.3. Simulations. The above convergence results are illustrated by some simulations. In Figure 5.1, we show two examples illustrating Proposition 5.1. Images are simulated using a perfect simulation method, see [42]. Gray levels are uniformly and independently drawn between 0 and 255 for each object. In the first example (left) we illustrate point (i); $\alpha = 2.5$, and $r_1 \to \infty$. The image is of size $10^3 \times 10^3$, $r_0 = 1$, $r_1 = 10^5$; the process converges to a constant field. In the second example (right), we illustrate point (ii); $\alpha = 3.5$, and $r_0 \to 0$. The image is of size $10^4 \times 10^4$, $r_0 = 1$, $r_1 = 10^4$; the process converges to white noise. In Figure 5.2 we illustrate the convergence of I_{r_0} when $r_0 \to 0$ and $\alpha = 2.9$. The first image is of size $10^4 \times 10^4$, $r_0 = 1$, $r_1 = 10^4$. The next three images are zooms on the same realization of the model (the zoom factor is two from one image to the next).

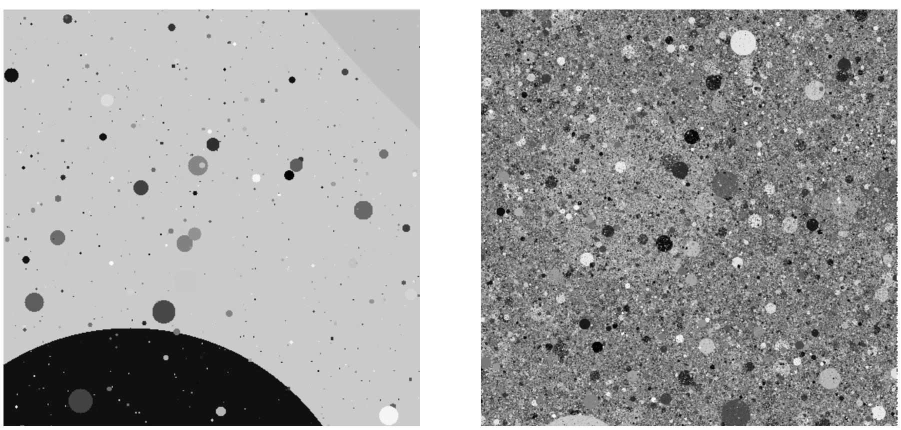

FIGURE 5.1. *Illustration of the degenerate cases of Proposition 5.1. Left: case (i), $\alpha < 3$ and $r_1 \to \infty$, the process converges to a constant (random) field. Right: case (ii), $\alpha > 3$ and $r_0 \to 0$, the process converges to a white noise.*

5.4. Preliminary properties of the limit field. For $\alpha \in (2, 3)$, Proposition 5.2(ii) shows that the bivariate distributions of I_0 given in Corollary 5.5 (taking the constant field for $\mathcal{C}$) exhibit interesting scaling properties. We have so far only been interested in finite-dimensional distributions of the colored dead leaves model. Let us now investigate how the scaling properties of the bivariate distributions influence the sample paths properties of the model. The first properties of the limit field that we may check are its stochastic continuity and the existence of a measurable version, whose definitions are recalled thereafter. A random field $\{Z(\mathbf{x}),\ \mathbf{x} \in \mathbb{R}^2\}$ is said

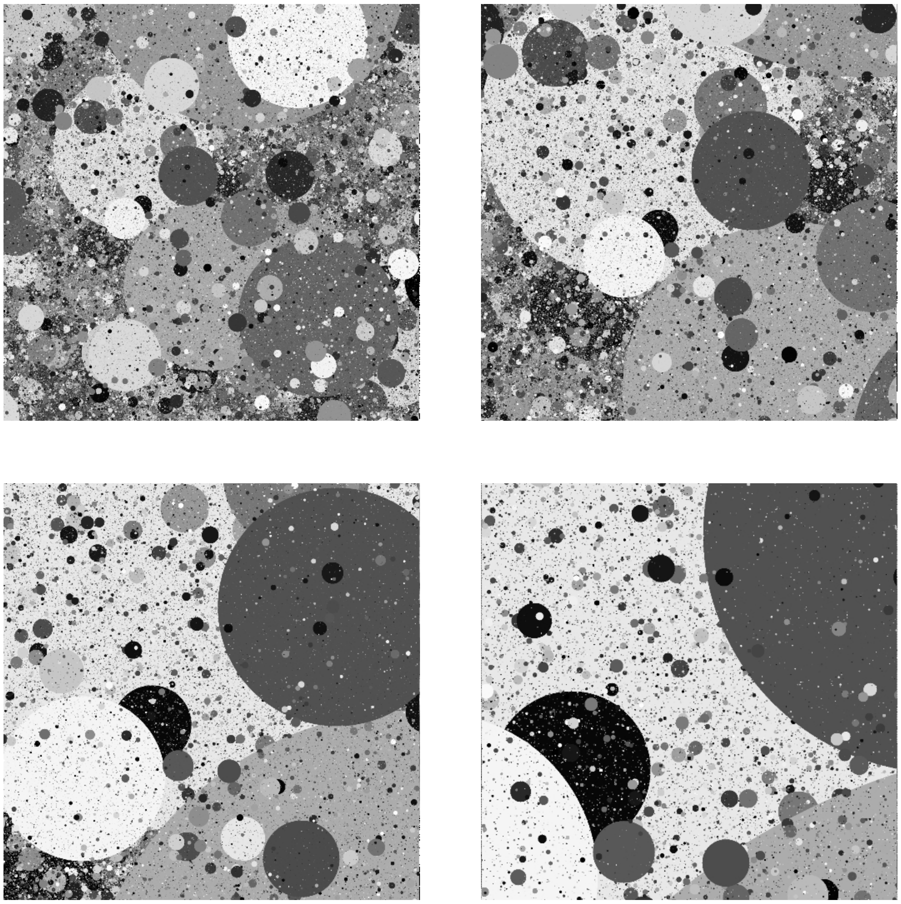

FIGURE 5.2. *Illustration of the convergence of the model when $\alpha = 2.9$ and $r_0 \to 0$. The first image (up left) is a realization when $r_0 = 1$, $r_1 = 10^4$, on a window of size $10^4 \times 10^4$. The next three images are zooms on this realization, the zoom factor being two from one image to the next.*

to be stochastically continuous if, for all $\mathbf{x} \in \mathbb{R}^2$, $Z(\mathbf{y}) \xrightarrow{\mathbb{P}} Z(\mathbf{x})$ ($Z(\mathbf{y})$ converges to $Z(\mathbf{x})$ in probability) as $\mathbf{y} \to \mathbf{x}$. A random field $\{\tilde{Z}(\mathbf{x}) : \mathbf{x} \in \mathbb{R}^2\}$ defined on $(\Omega, \mathcal{S}, \mathbb{P})$ is said to be a measurable version of Z if Z and $\tilde{Z}$ have same finite-dimensional distributions and $(\omega, \mathbf{x}) \mapsto \tilde{Z}(\omega, \mathbf{x})$ is a $(\Omega \times \mathbb{R}^2, \mathcal{S} \otimes \mathcal{B}(\mathbb{R}^2)) \to (\mathbb{R}, \mathcal{B}(\mathbb{R}))$ (jointly) measurable function (see e.g. [36, Section 9.4]).

PROPOSITION 5.6. *Take $\alpha \in (1, 3)$ and $r_1 < \infty$. Assume that $\mathcal{C}$ is stochastically continuous. Then $I_0^{\mathcal{C}}$ is stochastically continuous. If moreover $\mathcal{C}$ has a measurable version, then there exists a measurable version of $I_0^{\mathcal{C}}$.*

Proof. For convenience we write I for $I_0^{\mathcal{C}}$ in this proof. The bivariate distributions of I are given in Corollary 5.5. We have seen that $\mathbf{x} \mapsto p(0, r_1, \mathbf{x})$ defined by (5.3) is a continuous function. We obtain, for all $\mathbf{x}, \mathbf{y} \in \mathbb{R}^2$ and for all $\epsilon > 0$,

$$\mathbb{P}(|I(\mathbf{x}) - I(\mathbf{y})| > \epsilon) \leq \mathbb{P}(|\mathcal{C}(\mathbf{x}) - \mathcal{C}(\mathbf{y})| > \epsilon) + (1 - p(0, r_1, \mathbf{y} - \mathbf{x})),$$

which tends to zero as $\mathbf{y} \to \mathbf{x}$ for $\mathcal{C}$ stochastically continuous and since $p(0, r_1, 0) = 1$. Hence the first part of the proposition. For the second part, we apply [36, Theorem 9.4.2]. We have to check two conditions on I, namely

(i) There exists a countable set $S \subset \mathbb{R}^2$ such that for all $\mathbf{x} \in \mathbb{R}^2$, there exists a sequence $(\mathbf{x}_k)$ such that $I(\mathbf{x}_k) \xrightarrow{\mathbb{P}} I(\mathbf{x})$ as $k \to \infty$ and $\mathbf{x}_k \in S$ for all k.
(ii) For all $G, H \in \mathcal{B}(\mathbb{R})$ and for all $\mathbf{x} \in \mathbb{R}^2$, $\mathbf{y} \mapsto \mathbb{P}(I(\mathbf{x}) \in G, I(\mathbf{y}) \in H)$ is a $(\mathbb{R}^2, \mathcal{B}(\mathbb{R}^2)) \to ([0,1], \mathcal{B}([0,1]))$ measurable function.

Condition (i) is a consequence of stochastic continuity. Moreover, since $\mathcal{C}$ has a measurable version, it satisfies Condition (ii). This condition is then easily checked on I by using the bivariate distributions given in Corollary 5.5. □

As in the case $r_0 > 0$, we denote by I_0 the limit field in the case where $\mathcal{C}$ is the constant field with uniform marginals.

COROLLARY 5.7. *The colored dead leaves model I_0 is stationary, stochastically continuous and it admits a measurable version if and only if $\alpha \in (1,3)$.*

Proof. Stationarity follows from Remark 4. For $\alpha \geq 3$, I_0 is a white noise and thus does not have a measurable version (see [36, Example 9.4.3]) and neither is stochastically continuous. For $\alpha \in (1,3)$ the constant random field trivially satisfies the assumptions of Proposition 5.6. □

From now on, when $1 < \alpha < 3$, we will identify I_0 with its measurable version, and call it the *Scaling Dead Leaves* (SDL) model associated with the random set Y.

Natural images modeling. As explained in the introduction, the SDL enables to reproduce the scaling behaviors that are observed on natural images. Based on experiments reported in [34], [2] and [22], as well as experiments we performed using a statistical estimator introduced in [18] and relying on the variance of wavelet coefficients, most images can be modeled by a SDL with a value of α in $(2,3)$.

Next, we underline some qualitative properties of the stationary random field $I_0^{\mathcal{C}}$ that make it suitable for image modeling. First we emphasize that although this field is obtained as a limit it still enjoys a complicate "macro-structure" in its distributions, as suggested by Figure 5.2. This macro-structure is described in the context of colored tessellations in Appendix A, where the finite-dimensional distributions are computed by introducing a complex mixture structure (see (A.1)). This structure is preserved for $I_0^{\mathcal{C}}$ as shown by Corollary 5.5 in the particular case of bivariate distributions. For instance, if $\mathcal{C}$ is a constant field, any two distinct points $\mathbf{x}$ and $\mathbf{y}$ have the same color with probability $p(0, r_1, \mathbf{y} - \mathbf{x}) \in (0,1)$. Thus $I_0^{\mathcal{C}}$ has *homogeneous* regions in a weak sense (that is, despite the presence of small objects everywhere, see Lemma 4.3). Also recall that $I_0^{\mathcal{C}}$ has the same marginal distribution as $\mathcal{C}$. In particular, $I_0^{\mathcal{C}}$ may have Gaussian marginals with exactly the same geometrical structure. This would not be possible for a Gaussian field (that is a field not only with Gaussian marginals, but also with Gaussian finite-dimensional distributions) having the same covariance as $I_0^{\mathcal{C}}$. Note also that if h is an increasing function from $\mathbb{R}$ to $\mathbb{R}$ (a *contrast change*), then the field $h \circ I_0^{\mathcal{C}}$ has the same distribution as $I_0^{h \circ \mathcal{C}}$. In other words, the model $I_0^{\mathcal{C}}$ enables to independently control the contrast (through $\mathcal{C}$), and the geometry (through Y). This feature is inherited from the dead leaves model and is in agreement with the well known fact that the main visual information of a natural image is preserved under such a contrast change.

Convergence of digital images. We now briefly address the issue of the convergence of a sampled version of I_r. For all $r \in [0, r_1]$, we let J_r denote the random field defined on $[0,1]^2$ by integrating I_r, that is, for all $\mathbf{x} = (x_1, x_2) \in [0,1]^2$,

$$J_r(\mathbf{x}) = \iint_{\mathbf{y} \in [0,x_1] \times [0,x_2]} I_r(\mathbf{y})\, d\mathbf{y} \;.$$

Because I_r takes its values in $[0,1]$, it follows from Theorem 5.4 that

COROLLARY 5.8. *As r goes to 0 from above, J_r weakly converges to J_0 in the Banach space $\mathcal{C}([0,1]^2)$ of continuous functions on $[0,1]^2$ endowed with the uniform norm. That is, for any real-valued, bounded and continuous function g defined on this space, $g(J_r) \xrightarrow{\mathrm{d}} g(J_0)$.*

Proof. First, using Theorem 5.4 and the fact that I_r is bounded independently of r, one easily gets that $\mathbb{E}[J_r^{p_1}(\mathbf{x}_1)\dots J_r^{p_n}(\mathbf{x}_n)] \to \mathbb{E}[J_0^{p_1}(\mathbf{x}_1)\dots J_0^{p_n}(\mathbf{x}_n)]$ for any $n \geq 1$, any $\mathbf{x}_1,\dots,\mathbf{x}_n \in [0,1]^2$ and any positive integers $p_1,\dots,p_n$, which implies that $J_r \xrightarrow{\text{fidi}} J_0$. Second, using again that I_r is bounded, J_r is a 1-Lipschitz function taking its values in $[0,1]$ and hence lies in a fixed compact subset of $\mathcal{C}([0,1]^2)$. This provides a tightness condition ensuring the claimed functional weak convergence. ∎

Corollary (5.8) implies in particular that

$$< \phi, I_r >:= \int \phi(t) I_r(t)\, dt \xrightarrow{\mathrm{d}} \int \phi(t) I_0(t)\, dt \quad \text{as} \quad r \to 0\ ,$$

for any compactly supported functions ϕ such that, say by an integration by parts, $< \phi, I_r >= g(J_r)$ with g continuous and bounded on $\mathcal{C}([0,1]^2)$ (e.g. if ϕ is the indicator function of a rectangle, or if it is continuously differentiable). In the same way, for n such functions $\phi_1,\dots,\phi_n$, one gets the joint convergence of $\{< \phi_1, I_r >, \dots, < \phi_n, I_r >\}$ as $r \to 0$. If $(\mathbf{x}_1,\dots,\mathbf{x}_2)$ are n points in $[0,1]^2$ and for any $1 \leq i \leq n$, $\phi_i(\mathbf{x}) = \phi(\mathbf{x}_i - \mathbf{x})$ with ϕ a standard function with bounded support modeling the sensor of an imaging device, one gets the convergence of the digitization of I_r towards the digitization of I_0.

6. Sample paths properties. In this section, we investigate the regularity of I_{r_0} in both cases $r_0 > 0$ and $r_0 = 0$. We first note that the results below can be generalized to colored dead leaves processes $I_{r_0}^{\mathcal{C}}$ but, in general, they would depend on $\mathcal{C}$. Here we focus on the properties of the model that are only driven by the process R_{r_0}. Therefore we only consider the case of I_{r_0}, for which $\mathcal{C}$ is a constant field with uniform marginals. Similarly, the regularity of Y may influence the regularity of I_{r_0} (as in the example given at the end of Appendix C) but this will be avoided in our results by assuming (A-4).

These hypotheses on $\mathcal{C}$ and Y are not made only for technical simplicity. The main reason is that we want to understand how the smoothness of the image is influenced by the sole presence of small objects at all scales, even though these objects are not textured and have smooth boundaries. Finally, since we only take interest in local smoothness and since I_{r_0} is stationary, we may consider its restriction to the cube $[0,1]^2$ without loss of generality.

If $r_0 > 0$, the field I_{r_0} has paths for which occlusion influences the smoothness in a simple way. In short, it introduces discontinuities along $\partial M(r_0, r_1)$ and, within the interiors of the V_i's, the field is constant. This simple remark enables to state a first regularity property of I_{r_0}. Let us recall that the space BV of functions with bounded variation on $(0,1)^2$ is the set of integrable functions f such that

$$|f|_{BV} := \sup \left\{ \int f \operatorname{div}(\phi) \ :\ \phi \in \mathcal{C}_c^1((0,1)^2, \mathbb{R}^2) \quad \text{and} \quad \|\phi\|_\infty \leq 1 \right\} < \infty,$$

where $\mathcal{C}_c^1((0,1)^2, \mathbb{R}^2)$ is the set of $\mathcal{C}^1$ functions from $(0,1)^2$ to $\mathbb{R}^2$ with compact support in $(0,1)^2$. An important result that we will use below is that if A is a Borel set of $(0,1)^2$, then $|\mathbb{1}_A|_{BV} \leq \mathcal{H}^1(\partial A)$, where $\mathcal{H}^1$ denotes the one-dimensional Hausdorff measure on $\mathbb{R}^2$. In fact, an equality can be achieved using the more involved notion of measure theoretic boundary (see [14]) which is included in the topological boundary. The BV norm is defined as $\|f\|_{BV} := \|f\|_1 + |f|_{BV}$, where $\|\cdot\|_1$ denotes the usual L^1 norm on $(0,1)^2$. Since we only consider fields taking values in $[0,1]$, the L^1 part will always be bounded by one. In the simple case where ∂Y has finite length a.s., so have all boundaries of visible parts of $M(r_0, r_1)$ and since it is a tessellation, only a finite number of visible parts intersect $(0,1)^2$. It easily follows that I_{r_0} is locally of bounded variation a.s. Hereafter we provide a more formal proof and show the corresponding result in mean.

PROPOSITION 6.1. *Let r_0, r_1 and α be as in Proposition 4.1 (in which case the associated dead leaves model is well defined). Then I_{r_0} belongs to BV a.s. If moreover $E\mathcal{H}^1(\partial Y)$ is finite, then so is $\mathbb{E}\|I_{r_0}\|_{BV}$.*

Proof. Let $M = \sum_i \delta_{V_i}$ be the dead leaves model used for defining I_{r_0}, and ∂M its boundary. Applying the coarea formula (see [14]) and then the above mentioned bound on $|\mathbb{1}_A|_{BV}$, we get

$$\begin{aligned} |I_{r_0}|_{BV} &= \int_0^1 |\mathbb{1}_{\chi_\lambda}|_{BV}\, d\lambda \\ &\le \int_0^1 \mathcal{H}^1(\partial\chi_\lambda)\, d\lambda, \end{aligned}$$

where $\chi_\lambda = \{\mathbf{x} \in (0,1)^2 | I_{r_0}(\mathbf{x}) \ge \lambda\}$. Now, for all λ in $[0,1]$, $\partial\chi_\lambda \subset \partial M$. Indeed, pick a point $\mathbf{x}$ not in ∂M, then it is in the interior of a V_i. As the interior of this V_i has color $I_{r_0}(\mathbf{x})$, it is included in χ_λ for $\lambda \le I_{r_0}(\mathbf{x})$ and in its complementary set for $\lambda > I_{r_0}(\mathbf{x})$. Hence $\mathbf{x} \notin \partial\chi_\lambda$ for all $\lambda \in [0,1]$. Therefore we get that $|I_{r_0}|_{BV} \le \mathcal{H}^1(\partial M \cap (0,1)^2)$. The almost sure result then follows from Lemma B.2 of Appendix B. Moreover, by Lemma C.3, $E\mathcal{H}^1(\partial X) < \infty$, so that the result in mean also follows from Lemma B.2. □

This regularity result is in contradiction with empirical experiments. Indeed, in [17], by investigating the distribution of sizes of *bilevel* sets in natural images (up to the smallest available scale), it is shown that the bounded variation assumption fails to capture all the structure of images. In practice, a denoising approach relying on too smooth an *a priori* may interpret small objects as noise and, therefore, may result in a non-negligible loss of information. This is well known in image restoration, where variational methods in the space of functions with bounded variation, such as the famous Osher-Rudin denoising scheme, [35], are known to erase textured area. A recent approach to overcome this difficulty has been proposed by Y. Meyer, see [26], introducing a new functional space to account for textured regions in images. Here we take a different approach to the problem of modeling smoothness properties of natural images: we propose to derive smoothness spaces adapted to the (measurable) limit model I_0. We will take interest in Besov spaces and, as a byproduct, obtain that I_0 is not of bounded variation (at least in a mean sense), which is now coherent with the previously mentioned empirical results. Besov spaces provide a wide range of regularity spaces, and are adapted to the study of image processing tasks involving wavelets, such as compression and denoising, see e.g. [8]. Further insights about the links between the SDL, Osher-Rudin and Meyer models will be given in Section 7.

Before proceeding, let us mention another related approach, [28], where regularity notions for natural images are derived from a few basic assumptions. In particular, is is shown that the scale invariance assumption implies that images should be modeled as random distributions modulo constants. In contrast I_0 is a locally integrable random function (except in the white noise degenerate case), hence a more regular model. Of course these results are not contradictory, since I_0 is not scale invariant although it enjoys some self-similarity (see Proposition 5.2 : scale invariance would correspond to $\alpha = 3$ and exact power laws instead of approximations at small or large scales).

Of course not every value of α is relevant for the model I_0. First, the model is only defined for $\alpha < 3$. Moreover, based on previously mentioned empirical studies, we will only consider the case where $2 < \alpha < 3$. In fact for $\alpha \leq 2$ a change of behavior at small scales occurs, see Proposition 5.2 and Remark 3.

Let $s \in (0,1)$, $p \in [1,\infty]$ and $q \in [1,\infty]$. The Besov space $B_p^{s,q}$ (see e.g. [13]) is the Banach space endowed with the following norm

$$\|g\|_{B_p^{s,q}} := \|g\|_p + \left(\int_{u>0} \left(\omega(g,u)_p \, u^{-s} \right)^q \, \frac{du}{u} \right)^{\frac{1}{q}},$$

where $\|\cdot\|_p$ is the usual L^p norm on $(0,1)^2$ and $\omega(g,u)_p$ is the L^p modulus of smoothness of g at scale u, that is $\omega(g,u)_p := \sup_{|\mathbf{y}|<u} \|\Delta(g,\mathbf{y})\|_p$, where $\Delta(g,\mathbf{y})$ is the difference operator applied to g with step $\mathbf{y}$ on $(0,1)^2$, that is, the function $\mathbf{x} \mapsto (g(\mathbf{x}+\mathbf{y}) - g(\mathbf{x}))\mathbb{1}(\mathbf{x} \in (0,1)^2,\, \mathbf{x}+\mathbf{y} \in (0,1)^2)$.

Proposition 6.2. *Let $2 < \alpha < 3$, $0 < r_1 < \infty$ and assume (A-4). Then ,for all $p \in [1,\infty)$ and for all $s \in (0,1)$, we have*

$$\mathbb{E}\left[\|I_0\|_{B_p^{s,p}}^p \right] < \infty \Leftrightarrow s < \frac{3-\alpha}{p}. \tag{6.1}$$

Proof. In this proof we write $A \asymp B$ if there exists a constant c (possibly depending on the constants s, p, α, r_0, r_1 and γ) such that $\frac{1}{c}B \leq A \leq cB$. It is more convenient to use the modified modulus of smoothness

$$w(f,u)_p := \left((1 \vee u^{-2}) \int_{|\mathbf{y}|<u} \|\Delta(f,\mathbf{y})\|_p^p \, d\mathbf{y} \right)^{\frac{1}{p}}.$$

which satisfies $w(\cdot,\cdot)_p \asymp \omega(\cdot,\cdot)_p$ (see [13]). Because I_0 is measurable, we may use the Fubini Theorem. Hence

$$\mathbb{E}[\|I_0\|_{B_p^{s,p}}^p] \asymp \mathbb{E}[\|I_0\|_p]^p + \int_{u>0} \int_{|\mathbf{y}|<u} \mathbb{E}[\|\Delta(I_0,\mathbf{y})\|_p^p] \; (1 \vee u^{-2}) u^{-ps} \; d\mathbf{y} \, \frac{du}{u}.$$

From Corollary 5.5 we compute

$$\mathbb{E}[\|\Delta(I_0,\mathbf{y})\|_p^p] = \int_{\mathbf{x} \in (0,1)^2 \cap ((0,1)^2 - \mathbf{y})} \mathbb{E}|I_0(\mathbf{x}+\mathbf{y}) - I_0(\mathbf{x})|^p \, d\mathbf{x} \asymp 1 - p(0, r_1, \mathbf{y}).$$

Inserting this into the previous equation and using the definition of $p(0, r_1, \cdot)$ in (5.3), we obtain

$$\mathbb{E}[\|I_0\|_{B_p^{s,p}}^p] \asymp 1 + 2 \int_{u>0} \int_{|\mathbf{y}|<u\wedge 1} \frac{\int_0^{r_1} (\gamma(0) - \gamma(\mathbf{y}/v)) \, v^{2-\alpha} \, dv}{\int_0^{r_1} (2\gamma(0) - \gamma(\mathbf{y}/v)) \, v^{2-\alpha} \, dv} \, \frac{1 \vee u^{-2}}{u^{1+ps}} d\mathbf{y} \, du. \tag{6.2}$$

Lemma C.1 gives that $2\gamma(0) - \gamma(\mathbf{x}) \asymp \gamma(0)$ (independently of $\mathbf{x}$ in $\mathbb{R}^2$). Since $\alpha < 3$, the denominator in the RHS of (6.2) behaves as a constant, namely

$$\int_0^{r_1} (2\gamma(0) - \gamma(\mathbf{y}/v)) \, v^{2-\alpha} \, dv \asymp \gamma(0) r_1^{3-\alpha}/(3-\alpha). \tag{6.3}$$

Concerning the numerator, a change of variable gives, for all $\mathbf{y} \neq 0$,

$$\int_0^{r_1} (\gamma(0) - \gamma(\mathbf{y}/v))\, v^{2-\alpha}\, dv = |\mathbf{y}|^{3-\alpha} \int_0^{r_1/|\mathbf{y}|} [\gamma(0) - \gamma(\mathbf{y}/(|\mathbf{y}|t))]\, t^{2-\alpha}\, dt$$

Beside, since $2 < \alpha < 3$ and $\gamma(0) - \gamma(\mathbf{x}) \in ([0, \gamma(0)]$, we get, under (A-4),

$$\sup_{|\mathbf{z}|=1} \int_0^\infty (\gamma(0) - \gamma(\mathbf{z}/t))\, t^{2-\alpha}\, dt < \infty.$$

By (C.1), we have, for all $\mathbf{z}$ such that $|\mathbf{z}| = 1$ and for all $r \in (0, 1/(2a_2))$,

$$\int_0^r (\gamma(0) - \gamma(\mathbf{z}/t)))\, t^{2-\alpha}\, dt = \int_0^r \gamma(0)\, t^{2-\alpha}\, dt = \frac{\gamma(0)}{3-\alpha} r^{3-\alpha}.$$

Using again that $\gamma(0) - \gamma(\mathbf{x})$ is non-negative for all $\mathbf{x}$, the last three equations finally give

$$\int_0^{r_1} (\gamma(0) - \gamma(\mathbf{y}/v))\, v^{2-\alpha}\, dv \asymp |\mathbf{y}|^{3-\alpha} (|\mathbf{y}| \vee 1)^{\alpha-3}.$$

From (6.2), (6.3) and the last equation, we obtain

$$\mathbb{E}[\|I_0\|^p_{B_p^{s,p}}] \asymp 1 + \int_{u>0} \left(\int_{|\mathbf{y}|<u\wedge 1} |\mathbf{y}|^{3-\alpha}\, d\mathbf{y} \right) (1 \vee u^{-2}) u^{-ps} \frac{du}{u}.$$

Hence the result. ∎

It is well known that $B_1^{1,1} \subset BV \subset B_1^{1,\infty} \subset B_1^{s,1}$ for all $s \in (0,1)$ with corresponding inequalities (up to multiplicative constants) for the norms associated to these spaces. Therefore, as a consequence of Proposition 6.2, and in contrast with the case $r_0 > 0$ investigated in Proposition 6.1, we have that, as we anticipated before, for any $r_1 > 0$ and $\alpha \in (2,3)$, $\mathbb{E}\|I_0\|_{BV} = \infty$.

We conclude this section with an almost sure smoothness result immediately following from Proposition 6.2.

Corollary 6.3. *Let $2 < \alpha < 3$, $0 < r_1 < \infty$ and assume (A-4). Then, for all $p \in [1, \infty)$, for all $q \in [1, \infty]$ and for all $s \in (0,1)$, we have*

$$s < \frac{3-\alpha}{p} \Rightarrow I_0 \in B_p^{s,q} \ \textit{a.s.} \tag{6.4}$$

Proof. We simply use that if a non-negative random variable has finite expectation, it is necessary finite a.s. Then well known inclusions of Besov spaces give the claimed result for all $q \in [1, \infty]$. ∎

Remark 5. *The reverse implication for (6.4) cannot be deduced from Proposition 6.2 alone and remains an open question.*

7. Links with other functional regularity models. Regularity assumptions for natural images occur in several tasks of image processing, including image compression, denoising and more recently the decomposition of an image into a geometry and a texture components.

First, [12] relates the Besov regularity of an image to compression performances when using wavelet thresholding. In particular, by Corollary 6.3, this result can by applied to the SDL. Another interesting point of this paper concerns some experiments, based on empirical compression performances, suggesting that their test images belong to Besov spaces $B_p^{s,p}$ with specific values for s and p. These values are all compatible with the regularity of the SDL I_0 given by Proposition 6.2.

Following the first chapter of [26], noisy or textured images are modeled as a sum $f = u + v$, where u is the regular component of the image and v contains the noise and the texture. Many algorithms proposed for denoising or for the texture-geometry separation problem consist in extracting u from f by minimizing

$$\lambda \|f - \hat{u}\| + \|\hat{u}\|_* \tag{7.1}$$

in $\hat{u}$. The choice of the norms or quasi-norms $\|\cdot\|$ and $\|\cdot\|_*$, and of the weight $\lambda > 0$ for a given noise variance, are all related to regularity assumptions on the model $f = u + v$. For instance, in the Osher-Rudin algorithm, $\|\cdot\|$ is the squared L^2 norm and $\|\cdot\|_*$ is the BV norm. Variants for the norm $\|\cdot\|_*$ include the $B_1^{1,1}$ norm ([12]), the $B_1^{1,\infty}$ norm ([19]) or the Mumford-Shah functional ([29]).

The regularity properties of the random field I_0 given by Proposition (6.1) show that for the range of interest $2 < \alpha < 3$ and the above propositions for $\|\cdot\|_*$, one has $E[\|I_0\|_*] = \infty$. This indicates that in the denoising problem, if u is an image generated by our model with $2 < \alpha < 3$ and v is the noise, such variational methods will generally over-smooth the image.

In [26], Meyer also proposed variants for the norm $\|\cdot\|$ in (7.1), better adapted for modeling textures, see also [30, 4]. The idea here is to choose norms $\|\cdot\|$ that will be small for textures. Let us first remark that any type of textures can be artificially included in our model by coloring the objects with a textured random field, that is by considering $I_0^{\mathcal{C}}$ with $\mathcal{C}$ having a textured component. However, our interest again lies in the SDL model I_0 because it is textured as a result of the presence of objects at arbitrarily small scales. This is corroborated by the fact that $E[\|I_0\|_*] = \infty$ with the usual choices for the norm $\|\cdot\|_*$, implying that the random model I_0 should contain a texture component v. On the other hand, the regularity of the SDL is smoother than the one induced by the norm $\|\cdot\|$ that is usually chosen for the v component. This should not be interpreted as contradictory with the standard regularity assumptions used for the textured component v in the $u + v$ models. It only means that the regularity of I_0 lies somewhere between the regularities of u and v, see the following paragraph. The choice of the norm $\|\cdot\|$ is in fact driven by how one wants to model a texture. For instance, in [26], norms corresponding to spaces of function larger than L^2 are proposed, not because textures should not belong to L^2 but because norms $\|\cdot\|$ that are smaller than the L^2 norm on oscillating functions should be preferred.

We conclude by comparing the regularity of the SDL with another notion introduced by Y. Meyer as a generalization of the space BV in the context of image denoising. Theorem 15 in Section 21 of [26] characterizes the behavior of a variant of the Osher-Rudin functional by means of a wavelet expansion. More precisely, set, for any $\lambda > 0$,

$$\omega_\lambda(f) = \inf_{\hat{u}} \{\lambda \|f - \hat{u}\| + \|\hat{u}\|_*\} ,$$

with $\|\cdot\|$ being the L^2 norm (instead of the *squared* L^2 norm in the Osher-Rudin functional) and $\|\cdot\|_*$ being the BV norm. Then, this theorem says that, for any exponent $\gamma \in (0, 1)$, the interpolation norm

$$\|f\|_{(\gamma)} = \sup_{\lambda \geq 1} \lambda^{-\gamma} \omega_\lambda(f)$$

is finite if and only if the sorted (L^2 normalized) wavelet coefficients of f have a decreasing rate $n^{\gamma/2-1}$. Functional spaces defined by the norms $\|\cdot\|_{(\gamma)}$ for $\gamma \in (0,1)$ should be seen as interpolation spaces between L^2 and BV. The case $\gamma = 0$ would correspond to the BV space, and values of γ in $(0,1)$ define more irregular functional spaces, therefore offering a modeling alternative to the Besov spaces $B_q^{s,p}$. Using the wavelet characterization of Besov spaces, we obtain that if $E[\|I_0\|_{(\gamma)}] < \infty$ then $E[\|I_0\|_{B_1^{s,1}}] < \infty$ for any $s < 1-\gamma$, so that, by Proposition 6.2, $1-\gamma \leq 3-\alpha$, *i.e.*, $\gamma + \alpha \leq 2$. It would be interesting to check the following conjecture:

$$\|I_0\|_{(\gamma)} \text{ is finite a.s. if and only if } \gamma + \alpha \leq 2.$$

If true, it would give a characterization of α through the behavior of ω_λ as $\lambda \to \infty$.

8. A Bayesian prior. In addition to the functional regularity modeling investigated in Section 7, the limit dead leaves model can be used as a Bayesian prior. For elaborate tasks such as shape extraction, it is clear that the parameter α is not sufficient, and that geometrical properties of the model depending on the distribution of the shapes of objects have to be taken into account. In the context of denoising, the prior model I_0 has meaningful connexions with those introduced by [1] in the context of Bayesian wavelet shrinkage. More precisely, I_0 gives raise to mixture models for the jumps $I_0(\mathbf{x}) - I_0(\mathbf{y})$ in the image which are very close to those used for prior distributions on wavelet coefficients, namely a point mass at zero mixed with a standard unimodal density. The use of an SDL prior in the context of image denoising has been investigated in [18], where an estimate of the hyper-parameter α of the prior model I_0 is also proposed. There are few attempts ([32] or, more recently, [3]) to take some dependence structure of wavelet coefficients into account in the prior model. A direction for future work is to use the SDL I_0 as an alternative for modeling dependences within images.

9. Concluding remarks and open problems. In this paper, we investigated the implications on the small scales structure of natural images of both the occlusion phenomenon and the presence of scaling laws. This lead us to define a model, the scaling dead leaves, containing details at arbitrarily small scales. Several important issues remain to be tackled. First, the SDL relies on a simplified modeling of the formation of natural images. An important aspect of image formation that is not accounted for is the perspective effect. Indeed, the further the objects, the smaller they appear on the image, with a ratio given by the reciprocal of the distance. A very simple model in which all objects have the same size and lies on the ground, not taking occlusion into account, yields a distribution of sizes r^{-1} on the resulting image, thus a power distribution with a smaller value of α than those observed on natural images. A more realistic model consists in incorporating the perspective effect in the dead leaves model by defining its visible parts as

$$V_i := \left(\frac{\mathbf{x}_i + X_i}{t_i}\right) \setminus \left(\bigcup_{t_j \in (t_i, 0)} \left(\frac{\mathbf{x}_j + \overset{\circ}{X}_j}{t_j}\right)\right). \tag{9.1}$$

It is then of interest to investigate the regularity of such a model and in particular to compute the effect of perspective on the scaling properties of a potential limit model. Preliminary computations show that such a study requires a rescaling of the time axis to yield non-trivial results.

As mentioned earlier, another point concerns the use of the SDL as a prior in a denoising framework, initiated in [18], and which could benefit from either a better understanding of the dependence structure of wavelet coefficients or from an alternative approach using morphological filtering.

Finally, as detailed in Sections 6 and 7, several open questions remain concerning the functional regularity of the model and in particular its dual geometry-texture nature deserves further investigation.

Appendix A. Finite dimensional distribution of colored tessellations and their limits. Let T be an a.s. continuous random tessellation, $\mathcal{C}$ a random field and I the colored tessellation field associated to T and $\mathcal{C}$. Then the finite-dimensional distributions of I are mixtures of distributions only depending on the distribution of $\mathcal{C}$, with weights only depending on the distribution of the partition process R (see Definition 3.3). The following computations formalize this simple fact and provide explicit expressions of the mixture distributions.

Let $n \geq 1$ and $\mathbf{x_1}, \ldots, \mathbf{x_n}$ be n distinct points in $\mathbb{R}^d$. Since T is a.s. continuous, for all $\mathbf{x} \in \mathbb{R}^d$, we a.s. have $\sum_i \mathbb{1}(\mathbf{x} \in \overset{\circ}{F}_i) = 1$. Hence,

$$(I(\mathbf{x_1}), \ldots, I(\mathbf{x_n})) = \sum_{i_1, \ldots, i_n} (\mathcal{C}_{i_1}(\mathbf{x_1}), \ldots, \mathcal{C}_{i_n}(\mathbf{x_n})) \prod_{j=1}^{n} \mathbb{1}(\mathbf{x}_j \in \overset{\circ}{F}_{i_j}), \text{ a.s.}$$

We let $\mathcal{P}_n$ denote the set of all partitions of $\{1, \ldots, n\}$. For any indices $i_1, \ldots, i_n$ we define $K(i_1, \ldots, i_n)$ as the element of $\mathcal{P}_n$ such that l and m are in the same class of $K(i_1, \ldots, i_n)$ if and only if $i_l = i_m$. Reorganizing the sum above, we obtain, a.s.,

$$(I(\mathbf{x_1}), \ldots, I(\mathbf{x_n})) = \sum_{\kappa \in \mathcal{P}_n} \sum_{K(i_1, \ldots, i_n) = \kappa} (\mathcal{C}_{i_1}(\mathbf{x_1}), \ldots, \mathcal{C}_{i_n}(\mathbf{x_n})) \prod_{j=1}^{n} \mathbb{1}(\mathbf{x}_j \in \overset{\circ}{F}_{i_j}),$$

where the second sum is taken over all $(i_1, \ldots, i_n)$ such that $K(i_1, \ldots, i_n) = \kappa$. Since $T = \sum_i \delta_{F_i}$ is an a.s. continuous tessellation, only one product in this sum is non-zero in which case it is one, a.s. Using the independence of $\{\mathcal{C}_i\}$ with T, we then get that, for all $A \in \mathcal{B}(\mathbb{R}^n)$, $\mathbb{P}\left((I(\mathbf{x_1}), \ldots, I(\mathbf{x_n})) \in A\right)$ reads

$$\sum_{\kappa \in \mathcal{P}_n} \sum_{K(i_1, \ldots, i_n) = \kappa} \mathbb{P}\left((\mathcal{C}_{i_1}(\mathbf{x_1}), \ldots, \mathcal{C}_{i_n}(\mathbf{x_n})) \in A\right) \mathbb{P}\left(\bigcap_{j=1}^{n} \{\mathbf{x}_j \in \overset{\circ}{F}_{i_j}\}\right).$$

For all $\kappa \in \mathcal{P}_n$, we let κ_j denote the class of j in the partition κ. We let $\{\mathcal{C}_{\kappa,S} \,:\, \kappa \in \mathcal{P}_n, S \in \kappa\}$ be a collection of i.i.d. random fields on $\mathbb{R}^{\mathbb{R}^d}$ having the same distribution as $\mathcal{C}$ and independent of T. Then, for all n-tuple $(i_1, \ldots, i_n)$ such that $K(i_1, \ldots, i_n) = \kappa$, $(\mathcal{C}_{i_1}(\mathbf{x_1}), \ldots, \mathcal{C}_{i_n}(\mathbf{x_n}))$ has the same distribution as $(\mathcal{C}_{\kappa,\kappa_1}(\mathbf{x_1}), \ldots, \mathcal{C}_{\kappa,\kappa_n}(\mathbf{x_n}))$. Hence, for all $A \in \mathcal{B}(\mathbb{R}^n)$, $\mathbb{P}\left((I(\mathbf{x_1}), \ldots, I(\mathbf{x_n})) \in A\right)$ reads

$$\sum_{\kappa \in \mathcal{P}_n} \mathbb{P}\left((\mathcal{C}_{\kappa,\kappa_1}(\mathbf{x_1}), \ldots, \mathcal{C}_{\kappa,\kappa_n}(\mathbf{x_n})) \in A\right) \sum_{K(i_1, \ldots, i_n) = \kappa} \mathbb{P}\left(\bigcap_{j=1}^{n} \{\mathbf{x}_j \in \overset{\circ}{F}_{i_j}\}\right).$$

Using again that, a.s., there is a unique $(i_1, \ldots, i_n)$ such that $\mathbf{x}_j \in \overset{\circ}{F}_{i_j}$ for all $j = 1, \ldots, n$, we finally obtain that $(I(\mathbf{x_1}), \ldots, I(\mathbf{x_n}))$ is distributed as the finite mixture

$$\sum_{\kappa \in \mathcal{P}_n} \chi(\kappa; \mathbf{x_1}, \ldots \mathbf{x_n}) \, (\mathcal{C}_{\kappa,\kappa_1}(\mathbf{x_1}), \ldots, \mathcal{C}_{\kappa,\kappa_n}(\mathbf{x_n})), \tag{A.1}$$

where, for all $\kappa \in \mathcal{P}_n$,

$$\chi(\kappa; \mathbf{x_1}, \ldots \mathbf{x_n}) := \sum_{K(i_1,\ldots,i_n)=\kappa} \prod_{j=1}^{n} \mathbb{1}(\mathbf{x}_j \in \overset{\circ}{F}_{i_j}) \tag{A.2}$$

are random weights in $\{0, 1\}$ among which only one is nonzero, a.s.

Let us now determine $\chi(\kappa; \mathbf{x_1}, \ldots \mathbf{x_n})$ as a function of the process R. For this purpose, we use the partial order on $\mathcal{P}_n$ defined by

$$\kappa' \succeq \kappa \Longleftrightarrow \text{for all } S \in \kappa, \text{ there exists } S' \in \kappa' \text{ such that } S \subseteq S'.$$

We will write $\kappa' \succ \kappa$ if $\kappa' \succeq \kappa$ and $\kappa \neq \kappa'$. We first establish that, a.s., for all $\kappa \in \mathcal{P}_n$,

$$\prod_{S \in \kappa} \mathcal{R}(S) = \sum_{\kappa' \succeq \kappa} \chi(\kappa'; \mathbf{x_1}, \ldots \mathbf{x_n}), \tag{A.3}$$

where $\mathcal{R}(S)$ denote the (Bernoulli) random variable which takes value one if there exists i such that $S \subseteq \overset{\circ}{F}_i$ and takes value zero otherwise, that is,

$$\mathcal{R}(S) := \sum_i \prod_{\mathbf{x} \in S} \mathbb{1}(\mathbf{x} \in \overset{\circ}{F}_i) \ . \tag{A.4}$$

Note that the two sides of (A.3) are either zero or one. Suppose that the LHS is one. Then for all $S \in \kappa$, $\mathcal{R}(S) = 1$. By merging the sets S corresponding to the same F_i, we get a $\kappa' \succeq \kappa$ for which, applying (A.2) gives $\chi(\kappa'; \mathbf{x_1}, \ldots \mathbf{x_n}) = 1$. Hence the RHS of (A.3) also equals one. It can be similarly shown that if the LHS equals zero then the RHS does as well.

Having shown (A.3), an induction on $|\kappa|$ (the number of classes in the partition κ) shows that, for all $\kappa \in \mathcal{P}_n$, there exist weights $(w_{\kappa'})_{\kappa' \succ \kappa}$ in $\mathbb{Z}$ such that, a.s.,

$$\chi(\kappa; \mathbf{x_1}, \ldots \mathbf{x_n}) = \prod_{S \in \kappa} \mathcal{R}(S) + \sum_{\kappa' \succ \kappa} w_{\kappa'} \prod_{S \in \kappa'} \mathcal{R}(S). \tag{A.5}$$

The case where κ is the coarsest partition ($|\kappa| = 1$) is immediate from (A.3). The induction then relies on (A.3) and on the fact that $\kappa' \succeq \kappa$ implies either $\kappa = \kappa'$ or $|\kappa'| < |\kappa|$.

Now observe that, for all $m \geq 2$ and for all $\mathbf{y_1}, \ldots, \mathbf{y_m} \in \mathbb{R}^d$,

$$\mathcal{R}(\{\mathbf{y_1}, \ldots, \mathbf{y_m}\}) = \prod_{i=1}^{m-1} R(\mathbf{y_i}, \mathbf{y_{i+1}}). \tag{A.6}$$

Furthermore, we have, for all $\mathbf{y} \in \mathbb{R}^d$, $\mathcal{R}(\{\mathbf{y}\}) = R(\mathbf{y}, \mathbf{y}) = 1$ a.s. because T is assumed to be a.s. continuous. It then follows from (A.1), (A.5) and (A.6) that $(I(\mathbf{x_1}), \ldots, I(\mathbf{x_n}))$ is distributed as a finite mixture of distributions depending on the color field $\mathcal{C}$, with weights depending on the partition process R.

The preceding computations allow for simple conditions to let a sequence $(I_j)_{j \in \mathbb{N}}$ of colored tessellations converge to a limit field in the sense of finite-dimensional distributions.

Proposition A.1. *Consider a sequence of a.s. continuous random tessellations $(T_j)_{j \geq 0}$ and denote by R_j the partition process of T_j for all $j \geq 0$. Let $(\mathcal{C}_j = \{\mathcal{C}_j(\mathbf{x}) : \mathbf{x} \in \mathbb{R}^d\})_{j \geq 0}$ be a sequence of real valued random fields. Let us denote by I_j the colored tessellation process associated to T_j and $\mathcal{C}_j$ for all $j \geq 0$. Assume that*

(i) *there exists a random field R_∞ defined on $\mathbb{R}^d \times \mathbb{R}^d$ with values in $\{0,1\}$ such that $R_j \xrightarrow{\text{fidi}} R_\infty$.*

(ii) *there exists a real valued random field $\mathcal{C}_\infty$ defined on $\mathbb{R}^d$ such that $\mathcal{C}_j \xrightarrow{\text{fidi}} \mathcal{C}_\infty$.*

Then there exists a random field $\{I_\infty(\mathbf{x}) : \mathbf{x} \in \mathbb{R}^d\}$ such that $I_j \xrightarrow{\text{fidi}} I_\infty$. Furthermore the finite-dimensional distributions of I_∞ only depend on those of R_∞ and $\mathcal{C}_\infty$.

Proof. Take $n \geq 1$ and $\mathbf{x_1}, \dots, \mathbf{x_n}$ n distinct points in $\mathbb{R}^d$. From (i), (A.5) and (A.6), we have that the distribution of $\chi(\kappa; \mathbf{x_1}, \dots \mathbf{x_n})$ converges for all $\kappa \in \mathcal{P}_n$ as R_j converges to R_∞ and its limit distribution only depends on R_∞. From (ii), it follows that the finite mixture defined by (A.1) converges to a finite mixture defined by the distributions of R_∞ and $\mathcal{C}_\infty$. The result follows. ∎

The bivariate distributions of the limit can be directly derived from (3.3).

Proposition A.2. *Under the assumptions of Proposition A.1, for all $\mathbf{x}, \mathbf{y} \in \mathbb{R}^d$, the bivariate distribution $(I_\infty(\mathbf{x}), I_\infty(\mathbf{y}))$ is a mixture of $(\mathcal{C}_\infty(\mathbf{x}), \mathcal{C}_\infty(\mathbf{y}))$ and $(\mathcal{C}_\infty(\mathbf{x}), \mathcal{C'}_\infty(\mathbf{y}))$ with respective weights $\mathbb{P}(R_\infty(\mathbf{x}, \mathbf{y}) = 1)$ and $\mathbb{P}(R_\infty(\mathbf{x}, \mathbf{y}) = 0)$, where $\mathcal{C'}_\infty$ is an independent copy of $\mathcal{C}_\infty$.*

Of course, the bivariate distributions given above do not determine the distribution of I_∞. However, there are two degenerate cases for which the distribution of I_∞ is easily derived.

Corollary A.3. *Under the assumptions of Proposition A.1, consider the two following cases.*

(i) If, for all $\mathbf{x}$ and $\mathbf{y}$, $R_\infty(\mathbf{x}, \mathbf{y}) = 1$ a.s., then I_∞ has the same finite-distributions as $\mathcal{C}_\infty$.

(ii) If, for all $\mathbf{x} \neq \mathbf{y}$, $R_\infty(\mathbf{x}, \mathbf{y}) = 0$ a.s., then I_∞ has the same finite-distributions as a white noise with same marginals as $\mathcal{C}_\infty$.

Proof. As in the proof of Proposition A.1, we take $n \geq 1$ and $\mathbf{x_1}, \dots, \mathbf{x_n}$ n distinct points in $\mathbb{R}^d$. From this proof, we see that the finite-dimensional distributions of I_∞ are given by the finite mixture (A.1), where terms χ and $\mathcal{C}$ are replaced by their limits χ_∞ and $\mathcal{C}_\infty$. Similarly, weak limits can be taken in Equations (A.5) and (A.6), yielding equivalent relations with $\mathcal{R}_\infty(S)$ and χ_∞ replacing $\mathcal{R}(S)$ and χ.

Assume that, for all $\mathbf{x}, \mathbf{y} \in \mathbb{R}^d$, $R_\infty(\mathbf{x}, \mathbf{y}) = 1$ a.s. If κ is the partition consisting of a single class ($|\kappa| = 1$), (A.5) reads

$$\chi_\infty(\kappa; \mathbf{x_1}, \dots \mathbf{x_n}) = R_\infty(\{x_j, \, j = 1, \dots, n\}).$$

From (A.6), we see that $\chi_\infty(\kappa; \mathbf{x_1}, \dots \mathbf{x_n}) = 1$ for this κ (corresponding to $\kappa_1 = \dots = \kappa_n$), that is, the mixture (A.1) reduces to $(\mathcal{C}(\mathbf{x_1}), \dots, \mathcal{C}(\mathbf{x_n}))$.

Now assume that for all $\mathbf{x} \neq \mathbf{y} \in \mathbb{R}^d$, $R_\infty(\mathbf{x}, \mathbf{y}) = 0$ a.s.. Then by (A.6), $\mathcal{R}_\infty(\{\mathbf{y_1}, \dots, \mathbf{y_m}\}) = 0$, for all $m > 1$ and any m distinct points $\mathbf{y_1}, \dots, \mathbf{y_m}$ in $\mathbb{R}^d$. Let κ now denote the finest partition in $\mathcal{P}_n$ ($|\kappa| = n$). If $\kappa' \succ \kappa$, then there exists S in κ' such that $|S| > 1$, so that, by (A.5), $\chi_\infty(\kappa'; \mathbf{x_1}, \dots \mathbf{x_n}) = 0$. Therefore the mixture (A.1) reduces to $(\mathcal{C}_1(\mathbf{x_1}), \dots, \mathcal{C}_n(\mathbf{x_n}))$, where $\mathcal{C}_1, \dots, \mathcal{C}_n$ are i.i.d. copies of $\mathcal{C}$. ∎

Appendix B. Some results on the dead leaves model. In this section, we give two useful results for the dead leaves model defined in Section 3. We write $M = \sum \delta_{V_i}$ for the dead leaves model associated to a random closed set X satisfying Hypotheses (C-1), (C-2) and (C-3). We let $\Phi = \sum_i \delta_{\mathbf{x}_i, t_i, X_i}$ denote the point process on $\mathbb{R}^2 \times (-\infty, 0] \times \mathcal{F}'$ used to define M.

The following result was established in [6] and gives the probability that n compact sets are included in the interiors of distinct visible parts of a dead leaves model. It is a useful result to compute the finite dimensional distribution of the colored model.

PROPOSITION B.1. *Let $K_1, \dots, K_n$ be n non-empty compact sets. Define*

$$Q^{(n)}(K_1, \dots, K_n) := \mathbb{P}(\exists t_{i_1} < \dots < t_{i_n} : K_1 \subset \overset{\circ}{V}_{i_1}, \dots, K_n \subset \overset{\circ}{V}_{i_n}).$$

Let us denote

$$F^{(n)}(K_1, \dots, K_n) = E\nu(\overset{\circ}{X} \ominus \check{K}_1) \prod_{j=2}^{n} E\nu\left((\overset{\circ}{X} \ominus \check{K}_j) \cap (X \oplus \underline{\check{K}}_{j-1})^c \right), \tag{B.1}$$

and

$$G^{(n)}(K_1, \dots, K_n) = \prod_{j=1}^{n} E\nu\left(X \oplus \underline{\check{K}}_j\right), \tag{B.2}$$

where, for all j,

$$\underline{K}_j = \bigcup_{k=1}^{j} K_k. \tag{B.3}$$

Then

$$Q^{(n)}(K_1, \dots, K_n) = \frac{F^{(n)}(K_1, \dots, K_n)}{G^{(n)}(K_1, \dots, K_n)}. \tag{B.4}$$

For $n = 1$ we get the original result of Matheron, Formula (3.5).

An important feature of the dead leaves model is that, by construction, the boundary ∂M is a locally finite union of pieces of ∂X_is. The lemma below (that is needed to compute the expectation of the total variation of the colored dead leaves model) extends this idea by considering the expectation of the local length of this boundary.

LEMMA B.2. *Let M be the dead leaves model associated with a random set X, and K be a compact set. If $\mathcal{H}^1(\partial X)$ is finite a.s., then so is $\mathcal{H}^1(\partial M \cap K)$. Moreover, if $E\mathcal{H}^1(\partial X)$ is finite, then so is $\mathbb{E}\mathcal{H}^1(\partial M \cap K)$.*

Proof. Let K be a compact set of $\mathbb{R}^2$. By (C-2), we easily get, for all visible parts V_i (see (3.4)),

$$\partial V_i \subset (\mathbf{x}_i + \partial X_i) \cup \bigcup_{t_j \in (t_i, 0)} (\mathbf{x}_j + \partial X_j).$$

Since $\partial M \cap K = \cup_i \partial V_i \cap K$, and since the X_i's such that $V_i \cap K = \emptyset$ do not contribute to $\partial M \cap K$, we get

$$\partial M \cap K \subset \bigcup_{V_i \cap K \neq \emptyset} (\mathbf{x}_i + \partial X_i) \cap K. \tag{B.5}$$

Since M is a tessellation, it is a σ-finite measure on $\mathcal{F}'$ (see Section 3) so that $M(\mathcal{F}_K)$ (i.e. the number of visible parts V_i intersecting K) is finite a.s. for all compact sets K. Hence the first part of the lemma on the a.s. finiteness of $\mathcal{H}^1(\partial M \cap K)$.

We now bound its expectation. By stationarity of M, and using a finite covering of K by disks of radius r, it is sufficient to show that for all r such that $E\nu(X \ominus D(r)) > 0$ (e.g., by (C-3), $r \leq a$), the following bound holds true

$$\mathbb{E}\mathcal{H}^1(\partial M \cap D(r)) \leq \frac{\pi r^2 E\mathcal{H}^1(\partial X)}{E\nu(X \ominus D(r))}. \tag{B.6}$$

By definition of the visible parts V_i, we have

$$V_i \cap K \neq \emptyset \Rightarrow K \nsubseteq \bigcup_{t_j \in (t_i, 0)} (\mathbf{x}_j + \overset{\circ}{X}_j)$$
$$\Rightarrow \text{ for all } t_j \in (t_i, 0), K \nsubseteq (\mathbf{x}_j + \overset{\circ}{X}_j). \tag{B.7}$$

We define, for all $t \in (-\infty, 0)$, $x \in \mathbb{R}^2$ and $Y \in \mathcal{F}'$, the following nonnegative random variables

$$B_1(x, Y) := \mathcal{H}^1[(x + \partial Y) \cap K] \quad \text{and} \quad B_2(t, \Phi) := \prod_{t_j \in (t,0)} \mathbb{1}[K \nsubseteq (\mathbf{x}_j + \overset{\circ}{X}_j)].$$

Using these notations, and from (B.5) and (B.7), we obtain

$$\mathcal{H}^1(\partial M \cap K) \leq \sum_i B_1(\mathbf{x}_i, X_i)\, B_2(t_i, \Phi). \tag{B.8}$$

We now observe that Φ is a Poisson point process on $\mathbb{R}^2 \times (-\infty, 0] \times \mathcal{F}'$ with control measure μ equal to the Lebesgue measure on $\mathbb{R}^2 \times (-\infty, 0)$ multiplied by the probability distribution of X. Let us denote by $\mathbb{P}^u$ the Palm distribution of Φ at $u = (u_1, u_2, u_3)$. Applying the refined Campbell theorem (see [11]), we write

$$\mathbb{E} \sum_i B_1(\mathbf{x}_i, X_i)\, B_2(t_i, \Phi) = \int B_1(u_1, u_3)\, B_2(u_2, \phi)\, \mathbb{P}^u(d\phi)\, \mu(du).$$

Since Φ is Poisson, the Slivnyak's Theorem (see [41]) applies, giving, for all $u = (u_1, u_2, u_3) \in \mathbb{R}^2 \times (-\infty, 0] \times \mathcal{F}'$,

$$\int B_2(u_2, \phi)\, \mathbb{P}^u(d\phi) = \mathbb{E} B_2(u_2, \Phi + \delta_u) = \mathbb{E} B_2(u_2, \Phi),$$

where the last equality simply follows from the definition of B_2 above. Using the definition of μ and combining the last two equations, we get

$$\mathbb{E} \sum_i B_1(\mathbf{x}_i, X_i)\, B_2(t_i, \Phi) = \left(E \int_{\mathbb{R}^2} B_1(u_1, X)\, \nu(du_1) \right) \left(\int_{-\infty}^0 \mathbb{E} B_2(u_2, \Phi)\, du_2 \right). \tag{B.9}$$

Next we compute

$$\int B_1(u_1, X)\, \nu(du_1) = \mathcal{H}^1(\partial X) \nu(K); \tag{B.10}$$

$$\mathbb{E} B_2(u_2, \Phi) = \exp(u_2\, E \nu(X \ominus \check{K})). \tag{B.11}$$

Inserting these expressions in (B.9), (B.6) follows from (B.8) by taking $K = D(r)$, which will conclude the proof.

Equation (B.10) is a consequence of the following computation which relies on the translation invariance of $\mathcal{H}^1$ and ν, and on Fubini's Theorem,

$$\begin{aligned}\int \mathcal{H}^1[(u_1 + \partial X) \cap K]\, \nu(du_1) &= \int \mathcal{H}^1[\partial X \cap (K - u_1)]\, \nu(du_1) \\ &= \int \mathbb{1}(y + u_1 \in K)\, \mathbb{1}(y \in \partial X)\, \nu(du_1)\, \mathcal{H}^1(dy) \\ &= \mathcal{H}^1(\partial X) \nu(K).\end{aligned}$$

For computing (B.11), we note that the number of t_j's in $(u_2, 0)$ such that $K \subseteq (\mathbf{x}_j + X_j)$ (X_j may replace $\overset{\circ}{X}_j$ in the definition of B_2 using (C-2) and the fact that K is closed) is a Poisson random variable with parameter

$$E \int_{t=u_2}^{0} \int_{\mathbf{x} \in \mathbb{R}^2} \mathbb{1}\left[K \subseteq (\mathbf{x} + X)\right] dt\, d\mathbf{x} = -u_2\, E\nu(X \ominus \check{K}),$$

where we used that $K \subseteq (x + X)$ is equivalent to $-x \in X \ominus \check{K}$. This Poisson variable has probability $\exp(u_2\, E\nu(X \ominus \check{K}))$ to vanish. Hence (B.11). □

Appendix C. Regularity of γ at the origin. In this section, Y is a random closed set satisfying Assumption (A-1) and γ denotes its geometric covariogram. We now investigate the scope of validity of Assumption (A-4) in terms of the geometric properties of Y.

LEMMA C.1. *The function $\mathbf{y} \mapsto \gamma(\mathbf{y})$ is continuous over $\mathbb{R}^2$, $\gamma(0) \geq \pi a_1^2$ and, for all $\mathbf{y} \in \mathbb{R}^2$, $0 \leq \gamma(\mathbf{y}) \leq \gamma(0)$. Moreover,*

$$|\mathbf{y}| \geq 2a_2 \Rightarrow \gamma(\mathbf{y}) = 0, \tag{C.1}$$

where $|\cdot|$ is the Euclidean norm.

Proof. The bounds on γ are immediate. Now, $\mathbf{y} \mapsto \nu(Y \cap (\mathbf{y} + Y))$ is the convolution of the indicator function on Y with itself. Since Y is bounded, its indicator function is square integrable with respect to ν and the convolution is continuous. By the dominated convergence theorem, the continuity is preserved after taking the expectation. □

It is also known, see Proposition 4.3.1 in [25], that if Y is a deterministic convex set then $\gamma(\mathbf{x})$ has a one-sided derivative at $\mathbf{x} = 0$ in all directions. We now derive the following bound.

LEMMA C.2. *Let K be a compact set. Then for all $\mathbf{x} \in \mathbb{R}^2$,*

$$0 \leq \nu(\overset{\circ}{K}) - \nu(\overset{\circ}{K} \cap (\mathbf{x} + \overset{\circ}{K})) \leq \nu\left(\partial K \oplus [0, \mathbf{x}]\right),$$

where $[0, \mathbf{x}]$ denotes the segment $\{\alpha\mathbf{x},\, \alpha \in [0,1]\}$. In particular, if, for all $\delta > 0$, as $\mathbf{x} \to 0$,

$$E\nu\left(\partial Y \oplus [0, \mathbf{x}]\right) = o(|\mathbf{x}|^{1-\delta}),$$

then (A-4) holds true.

Proof. Let $\mathbf{x} \in \mathbb{R}^2$. We may write

$$0 \leq \nu(\overset{\circ}{K}) - \nu(\overset{\circ}{K} \cap (\mathbf{x} + \overset{\circ}{K})) = \nu(\overset{\circ}{K} \backslash (\mathbf{x} + \overset{\circ}{K}))$$

Let $\mathbf{y} \in \overset{\circ}{K} \backslash (\mathbf{x} + \overset{\circ}{K})$, that is $\mathbf{y} \in \overset{\circ}{K}$ and $\mathbf{y} - \mathbf{x} \notin \overset{\circ}{K}$. Thus the line segment $[\mathbf{y}, \mathbf{y} - \mathbf{x}]$ intersects ∂K, and the claimed bound follows. The sufficient condition for having (A-4) is then obtained by taking expectations. □

The obtained criterion imposed on ∂Y in order to satisfy (A-4) can be further simplified by using classical tools of measure theory. In the following result, we use the Hausdorff measure $\mathcal{H}^1$. We will then consider the box-counting dimension, and finally conclude this section by providing a simple example for which (A-4) does not hold.

LEMMA C.3. *Take r_0, r_1 and α as in Proposition 4.1. Assume that $E\mathcal{H}^1(\partial Y)$ is finite. Then, so is $E\mathcal{H}^1(\partial X)$ and (A-4) holds true. More precisely, we have, as $\mathbf{x} \to 0$, $\gamma(\mathbf{x}) = \gamma(0) + O(|\mathbf{x}|)$.*

Proof. Notice that $E\mathcal{H}^1(\partial X) = E[R\mathcal{H}^1(\partial Y)] = E(R)E\mathcal{H}^1(\partial Y)$. Under the conditions on r_0, r_1 and α assumed in Proposition 4.1, it is easily checked that $E(R)$ is finite. Hence the finiteness of $E\mathcal{H}^1(\partial X)$. Using that ν coincides with the Hausdorff measure $\mathcal{H}^2$ on Borel sets, it is easily shown that, for all Borel set K, $\nu\left(\partial K \oplus [0, \mathbf{x}]\right)$ is at most $|\mathbf{x}|\mathcal{H}^1(\partial K)$. Inserting this into the bound established in Lemma C.2, we find $0 \le \gamma(0) - \gamma(\mathbf{x}) \le |\mathbf{x}|E\mathcal{H}^1(\partial X)$. The result follows. □

We now mention a different bound applying in a case where $\mathcal{H}^1(\partial Y)$ is not necessary finite. For any closed set K, $\nu\left(\partial K \oplus [0, \mathbf{x}]\right)$ may be bounded by relying on the upper box-counting dimension of ∂K rather than its Hausdorff measure $\mathcal{H}^1$. Indeed, if this dimension is at most one, then (see [15, Proposition 3.2]), for all $\delta > 0$, as $x \to 0$,

$$\nu\left(\partial K \oplus D(x)\right) = o(x^{1-\delta}),$$

$D(x)$ being as before the disk of radius x centered at the origin. Of course $\nu\left(\partial K \oplus [0, \mathbf{x}]\right)$ is smaller than $\nu\left(\partial K \oplus D(x)\right)$ and, by Lemma C.2, this bound can be used to insure (A-4).

Finally, in order to illustrate that some smoothness is needed on the boundary of Y to insure (A-4), even for a deterministic Y, consider the following example. Let h be a continuous function defined on $[0, 1]$ and let us define

$$K := \left\{(x, y) : 0 \le x \le 1,\ h(x) - 1 \le y \le h(x)\right\}.$$

In particular, the boundary of K is made of two copies of the graph of h connected at their end points by two unit vertical segments. Beside, for all $u \in (0, 1)$, letting $\mathbf{e}_1$ denote the horizontal unit vector, a straightforward computation yields

$$\nu(\mathring{K}) - \nu(\mathring{K} \cap (u\mathbf{e}_1 + \mathring{K})) = \nu(\mathring{K} \backslash (u\mathbf{e}_1 + \mathring{K})) = u + \int_u^1 |h(x) - h(x-u)|\, dx.$$

Hence in this case, taking say $Y = K$ non-random (it could be made random by taking h random), (A-4) would imply that, for all positive δ, $\int_u^1 |h(x) - h(x-u)|\, dx = o(u^{1-\delta})$ as $u \to 0$. This is equivalent to saying that h belongs to all Besov spaces $B_p^{s,q}$ on $(0, 1)$ with $p = 1$, $q = \infty$ and $s < 1$ (we provide the definition of Besov spaces on $(0, 1)^2$ in Section 6; the definition on $(0, 1)$ is similar, see [13]). Now, it is known that there are continuous (even Hölder) functions h out of $B_1^{s,\infty}(0, 1)$ for any positive s. Choosing a continuous h out of $B_1^{s,\infty}(0, 1)$ for some $s \in (0, 1)$, we deduce that the corresponding Y do not satisfy (A-4). Moreover, in this precise example where the boundary of Y is constructed as a graph of a function, we see that Assumption (A-4) is equivalent to precise smoothness assumptions on this function.

Appendix D. Technical proofs.

D.1. Proof of Proposition 5.1.. Case (i) : Take $1 < \alpha < 3$ and $\mathbf{x} \in \mathbb{R}^2$. From Lemma C.1 and since, by (A-1), $\gamma(0) > 0$, for any $\epsilon > 0$, there exists u_0 such that for all $u \in [u_0, \infty)$,

$$|\gamma(\mathbf{x}/u) - \gamma(0)| \le \epsilon\gamma(0).$$

Since the integral $\int_{r_0}^{r_1} u^{2-\alpha}\,du$ diverges as $r_1 \to \infty$ and is bounded as $r_0 \to 0$, for r_1 sufficiently large and for all $r_0 \le r_1$,

$$\int_{r_0}^{r_1} u^{2-\alpha}\,du \le (1+\epsilon)\int_{u_0 \vee r_0}^{r_1} u^{2-\alpha}\,du.$$

From the last two equations and from (5.2), we get, for all r_1 sufficiently large and for all $0 < r_0 < r_1$,

$$1 \ge p(r_0, r_1, \mathbf{x}) \ge \frac{\gamma(0)(1-\epsilon)\int_{u_0\vee r_0}^{r_1} u^{2-\alpha}\,du}{\gamma(0)(1+\epsilon)^2\int_{u_0\vee r_0}^{r_1} u^{2-\alpha}\,du} = \frac{1-\epsilon}{(1+\epsilon)^2}.$$

Hence (i) by letting ϵ decrease to zero.

Case (ii) : Take $\alpha > 3$. From Lemma C.1 and (5.2), we have, for all $r_0 < r_1 \le |\mathbf{x}|/(2a_2)$, $p(r_0, r_1, \mathbf{x}) = 0$ and, for all $r_0 \le |\mathbf{x}|/(2a_2) < r_1$,

$$\int_{r_0}^{r_1} \gamma(\mathbf{x}/u)u^{2-\alpha}\,du = \int_{|\mathbf{x}|/(2a_2)}^{r_1} \gamma(\mathbf{x}/u)u^{2-\alpha}\,du.$$

Since γ is bounded by πa_2 from above, we get, for all $r_0 \le |\mathbf{x}|/(2a_2)$ and for all $r_1 > r_0$,

$$p(r_0, r_1, \mathbf{x}) \le \frac{\pi a_2 \int_{|\mathbf{x}|/(2a_2)}^{\infty} u^{2-\alpha}\,du}{2\gamma(0)\int_{r_0}^{|\mathbf{x}|/(2a_2)} u^{2-\alpha}\,du - \pi a_2\int_{|\mathbf{x}|/(2a_2)}^{\infty} u^{2-\alpha}\,du}$$

which does not depend on r_1 and tends to zero as $r_0 \to 0$. This gives (ii).

Case (iii) : Let $\alpha = 3$. From (C.1) and the continuity of γ, the numerator of the RHS of (5.2) behaves as $\gamma(0)\log(r_1)$ when r_0 and r_1 respectively tend to 0 and ∞. For the same reasons, the denominator behaves as $\gamma(0)(\log(r_1) - 2\log(r_0))$. We obtain (iii).

Case (iv) : The limit (5.3) is an immediate application of (5.2) by observing that γ is bounded (see Lemma C.1). Continuity of $\mathbf{x} \to p(0, r_1, \mathbf{x})$ follows from the continuity of γ and dominated convergence. ∎

D.2. Proof of Proposition 5.2.. Take $\alpha > 3$. An obvious change of variable gives

$$\int_{r_0}^{\infty} \gamma(x/u)u^{2-\alpha}\,du = x^{3-\alpha}\int_{r_0/x}^{\infty} \gamma(1/v)v^{2-\alpha}\,dv.$$

Using (C.1) and (5.2), letting $x/r_0 \to \infty$ gives (i). We now take $\alpha < 3$. We similarly have

$$\int_{0}^{r_1} (\gamma(x/u) - \gamma(0))u^{2-\alpha}\,du = x^{3-\alpha}\int_{0}^{r_1/x} (\gamma(1/v) - \gamma(0))v^{2-\alpha}\,dv.$$

From (5.2) and (5.3) and standard computations, we obtain (ii). ∎

REFERENCES

[1] F. Abramovich, T. Sapatinas, and B. W. Silverman, *Wavelet thresholding via a Bayesian approach*, J. R. Stat. Soc. Ser. B Stat. Methodol., 60 (1998), pp. 725–749.

[2] L. Alvarez, Y. Gousseau, and J.-M. Morel, *The size of objects in natural and artificial images*, Advances in Imaging and Electron Physics, Academic Press, 111 (1999), pp. 167–242.
[3] G. K. Ambler and B. W. Silverman, *Perfect simulation for bayesian wavelet thresholding with correlated coefficients*. Submitted, 2004.
[4] J.-F. Aujol, G. Aubert, L. Blanc-Fraud, and A. Chambolle, *Image decomposition into a bounded variation component and an oscillating component*, Journal of Mathematical Imaging and Vision, 22 (2005), pp. 71–88.
[5] P. Billingsley, *Convergence of Probability Measures*, Wiley, 1968.
[6] C. Bordenave, Y. Gousseau, and F. Roueff, *The dead leaves model : an example of a general tessellation*, Advances in Applied Probability, 38 (2006), pp. 31–46.
[7] E. J. Candès, *Ridgelets and their derivatives: Representation of images with edges*, in Curves and Surfaces, L. L. S. et al., ed., 1999.
[8] A. Chambolle, R. A. DeVore, N.-Y. Lee, and B. J. Lucier, *Nonlinear wavelet image processing: Variational problems, compression, and noise removal through wavelet shrinkage*, IEEE Transactions on Image Processing, 7 (1998), pp. 319–355.
[9] Z. Chi, *Probability Models for Complex Systems*, PhD thesis, Brown University, 1998.
[10] R. Cowan and A. K. L. Tsang, *The falling leaf mosaic and its equilibrium properties*, Advances in Applied Probability, 26 (1994), pp. 54–62.
[11] D. J. Daley and D. Vere-Jones, *An Introduction to the Theory of Point Processes*, Springler Verlag, 1988.
[12] R. DeVore and B. J. Lucier, *Fast wavelet techniques for near optimal image compression*, IEEE Mil. Com. Conf., (1992), pp. 1129–1135.
[13] R. A. DeVore and G. G. Lorentz, *Constructive approximation*, vol. 303 of A series of comprehensive studies in Mathematics, Springer-Verlag, 1991.
[14] L. C. Evans and R. F. Gariepy, *Measure Theory and Fine Properties of Functions.*, Studies in Advanced Math., CRC Press, 1992.
[15] K. J. Falconer, *Fractal Geometry: Mathematical Foundations and Applications*, John Wiley and Sons, New York, 1990.
[16] S. Geman and D. Geman, *Stochastic relaxation, Gibbs distribution, and the Bayesian restoration of images.*, IEEE Trans. on Pattern Analysis and Machine Intelligence, (1984), pp. 721–741.
[17] Y. Gousseau and J.-M. Morel, *Are natural images of bounded variation?*, SIAM J. Math. Analysis, 33 (2001), pp. 634–648.
[18] Y. Gousseau and F. Roueff, *A geometric a priori for capturing the regularity of images*, in EUSIPCO 05, 2005.
[19] A. Haddad and Y. Meyer, *Variational methods in image processing*, Tech. Rep. 08, CMLA, ENS-Cachan, 2005.
[20] J. Huang and D. Mumford, *Statistics of natural images and models*, Proc IEEE Conf. Computer Vision and Pattern Recognition, (1999), pp. 541–547.
[21] D. Jeulin, *Dead leaves models: From space tesselation to random functions*, in Advances in Theory and Applications of Random Sets, D. Jeulin, ed., 1996.
[22] A. Lee, D. Mumford, and J. Huang, *Occlusion models for natural images: A statistical study of a scale invariant dead leaves model*, Int'l J. of Computer Vision, 41 (2001), pp. 35–59.
[23] N. N. Lyashenko, *Statistics of random compacts in the euclidean space*, J. Soviet. Math., 21 (1983), pp. 76–92.
[24] G. Matheron, *Modèle séquentiel de partition aléatoire*, tech. rep., CMM, 1968.
[25] ———, *Random Sets and Integral Geometry*, John Wiley & Sons, New York, 1975.
[26] Y. Meyer, *Oscillating patterns in image processing and nonlinear evolution equations*, vol. 22 of University Lecture Series, American Mathematical Society, Providence, RI, 2001. The fifteenth Dean Jacqueline B. Lewis memorial lectures.
[27] I. Molchanov, *Limit Theorems for Unions of Random Closed Sets*, vol. 1561 of Lecture Notes in Mathematics, Springer Verlag, 1993.
[28] D. Mumford and B. Gidas, *Stochastic models for generic images*, Quaterly Journal of Mathematics, 59 (2001), pp. 85–111.
[29] D. Mumford and J. Shah, *Boundary detection by minimizing functionals*, in IEEE Conference on Computer Vision and Pattern Recognition, 1985, pp. 22–26.
[30] S. Osher, A. Sole, and L. Vese, *Image decomposition and restoration using total variation minimization and the h^{-1} norm*, SIAM Multiscale Modeling and Simulation, 1 (2003), pp. 349–170.
[31] E. L. Pennec and S. Mallat, *Bandelet image approximation and compression*, SIAM Multiscale Modeling and Simulation, 4 (2005), pp. 992–1039.

[32] J. Romberg, C. H., and R. Baraniuk, *Bayesian tree-structured image modeling using wavelet-domain hidden markov modelsw*, IEEE Transactions on Image Processing, 10 (2001), pp. 1056–1068.
[33] D. L. Ruderman, *The statistics of natural images.*, Network: Computation in Neural Systems, 5 (1994), pp. 517–548.
[34] ———, *Origins of scaling in natural images.*, Vision Research, 37 (1997), pp. 3385–3398.
[35] L. Rudin, S. Osher, and E. Fatemi, *Nonlinear total variation based noise removal algorithms.*, Physica D, 60 (1992), pp. 259–268.
[36] G. Samorodnitsky and M. S. Taqqu, *Stable non-Gaussian processes: stochastic models with infinite variance*, Chapman and Hall, 1994.
[37] J. Serra, *Image Analysis and Mathematical Morphology*, Academic Press, London, 1982.
[38] E. P. Simoncelli, *Statistical model for images: Compression, restoration and synthesis.*, in 31st Asilomar Conference on Signal, Systems and Computers, 1997.
[39] A. Srivastava, A. B. Lee, E. P. Simoncelli, and S.-C. Zhu, *On advances in statistical modeling of natural images*, Journal of Mathematical Imaging and Vision, 18 (2003), pp. 17–33.
[40] D. Stoyan, *On generalized planar tessellation*, Math. Nachr., 128 (1986), pp. 215–219.
[41] D. Stoyan, W. S. Kendall, and J. Mecke, *Stochastic Geometry and its Applications*, Wiley Series in Probability and Statistics, Wiley, 2nd ed., 1995.
[42] E. Thonnes and W. S. Kendall, *Perfect simulation in stochastic geometry*, Pattern Recognition, 32 (1999), pp. 1569–1586.
[43] G. Winkler, *Image Analysis, Random Fields and Dynamic Monte Carlo Methods*, Springer-Verlag, 1995.